Adaptive Nonlinear Incremental Flight Control for Systems with Unknown Control Effectiveness

Chang, Jing; De Breuker, Roeland; Wang, Xuerui

DOI
10.1109/TAES.2022.3187057

Publication date
2022

Document Version
Final published version

Published in
IEEE Transactions on Aerospace and Electronic Systems

Adaptive Nonlinear Incremental Flight Control for Systems With Unknown Control Effectiveness

JING CHANG
Xidian University, Xi'an, China
Delft University of Technology, Delft, The Netherlands

ROELAND DE BREUKER
XUERUI WANG, Member, IEEE
Delft University of Technology, Delft, The Netherlands

This article exposes that although some sensor-based nonlinear fault-tolerant control frameworks including incremental nonlinear dynamic inversion control can passively resist a wide range of actuator faults and structural damage without requiring an accurate model of the dynamic system, their stability heavily relies on a sufficient condition, which is unfortunately violated if the control direction is unknown. Consequently, it is proved in this article that no matter, which perturbation compensation technique (adaptive, disturbance observer, sliding-mode) is implemented, none of the existing nonlinear incremental control methods can guarantee closed-loop stability. Therefore, this article proposes a Nussbaum function-based adaptive incremental control framework for nonlinear dynamic systems with partially known (control direction is unknown) or even completely unknown control effectiveness. Its effectiveness is proved in the Lyapunov sense and is also verified via numerical simulations of an aircraft attitude tracking problem in the presence of sensing errors, parametric model uncertainties, structural damage, actuator faults, as well as inversed and unknown control effectiveness.

Manuscript received 17 March 2022; revised 6 May 2022; accepted 13 June 2022. Date of publication 28 June 2022; date of current version 10 February 2023.

DOI. No. 10.1109/TAES.2022.3187057

Refereeing of this contribution was handled by H. Alwi.

This work was supported by the National Natural Science Foundation of China under Grant 62003252 and Grant 62073254.

Authors' addresses: Jing Chang is with the School of Aerospace Science and Technology, Xidian University, Xi'an 710126, China and also with the Faculty of Aerospace Engineering, Delft University of Technology, 2629HS Delft, The Netherland, E-mail: (j.chang-2@tudelft.nl); Roeland De Breuker and Xuerui Wang are with the Faculty of Aerospace Engineering, Delft University of Technology, 2629HS Delft, The Netherland, E-mail: (r.debreuker@tudelft.nl; X.Wang-6@tudelft.nl). *(Corresponding author: Xuerui Wang.)*

I. INTRODUCTION

Nonlinear fault-tolerant control (FTC) is promising for enhancing flight safety [1]–[4]. Among all the FTC methods in the literature, the nonlinear incremental control has drawn much attention because of its data-driven and sensor-based features [1]. By exploiting sensor measurements, nonlinear incremental control can passively tolerant various uncertainties, actuator faults, external disturbances, and even structural damage without requiring an accurate model of the controlled vehicle [5], [6]. This property is promising for aerospace systems that are subjected to nonlinearities, uncertainties, and various sources of disturbances. In addition, nonlinear incremental control is one of the effective and easy to implement control techniques, which has been shown by quadrotor flight tests [7] and even CS–25 certified passenger aircraft flight tests [8].

The only model information needed by nonlinear incremental control is the control effectiveness matrix (CEM). However, the accurate estimation of CEM is challenged by uncertainties (both parametric and nonparametric), nonlinearities, external disturbances, and unknown fault modes [9]. Moreover, when designing the incremental control methods, the higher-order expansion reminders and state variation-related terms are typically neglected. However, in the closed-loop system, they still remain, influencing the performance and stability [10]. Therefore, it is important to energize nonlinear incremental control with active online perturbation compensation ability. In the literature, there are mainly three effective approaches for achieving this goal: adaptive augmentation [6], [11], observer augmentation [7], [12], and sliding-mode compensation [5].

Analyzing the closed-loop stability and robustness of the nonlinear incremental control framework with these three augmentation approaches is an active research area. Recently, control gain-dependent stability conditions for incremental backstepping under perturbations are derived in [13] using linear transfer functions. However, only single input systems are addressed. In [12], Lyapunov-based stability proof is derived for nonlinear incremental control with adaptation augmentation under the assumption of bounded model uncertainties and their derivatives. Moreover, the closed-loop stability under sliding mode control augmented nonlinear incremental control is proved in the Lyapunov sense [5]. This proof requires a sufficient condition on the estimation of CEM. Furthermore, an analogous approach is used to prove a sliding mode disturbance observer augmented nonlinear incremental control in [7]. The feasibility of incremental control encountering control reversal is questioned in [10]. A control direction-based incremental sliding mode control is also proposed to expand the applicability of incremental control. However, this method relies on a strong assumption that the information of control reversal is already available.

The discussions above reveal that the existing stability and robustness analysis approaches for the nonlinear incremental control depend on the specific augmentation technique. Despite the augmentation techniques, a unified

stability proof in the Lyapunov framework for multi-input–multi-output (MIMO) nonlinear perturbed systems is desirable. Furthermore, the unknown control direction is considered one of the most difficult issues facing in FTC design. Regarding flight control, this challenge can be caused by aeroelasticity [14], hardware connection errors [15], pilot errors [16], etc. However, none of the existing nonlinear incremental control methods has addressed this challenge. Their stability criteria are also violated in the presence of unknown control direction.

Typically, aerospace dynamic systems are MIMO. However, tackling the unknown control direction challenge of the MIMO systems is still an open research challenge [17], [18]. Focusing on the single/double-integrator multiagents with unknown and nonidentical control directions, a new distributed nonlinear proportional-integral-based control law has been provided in [19]. However, this approach is not suitable for MIMO systems. Robust sliding mode output-feedback controllers using monitoring function are developed for uncertain linear systems [20] and nonlinear systems [21] with unknown CEM. However, they assume that the CEM elements are constant in these monitoring functions. A multiple-model adaptive switching control scheme is proposed in [22]. The multiple-model adaptive control with a switching scheme based on normalized estimation errors addresses the challenge of multiple unknown control direction. For a p-input q-output system, this approach needs in total 2^p controllers and 2^p estimators.

Another approach to address the unknown control direction challenge is the Nussbaum gain approach embedded in adaptive control design [23]–[25]. However, there is a significant obstacle preventing the applicability of conventional Nussbaum functions in MIMO systems: the involvement of multiple Nussbaum functions is unavoidable, but unfortunately, their effects may counteract each other [24], [26]. Several Type-B Nussbaum functions with different frequencies that allow the addition of multiple Nussbaum functions within a single inequality are proposed to solve this issue [24], [26]–[28]. Since the aircraft dynamics are MIMO with a nondiagonal CEM, the features of Type-B Nussbaum functions make them promising for solving fault-tolerant flight control problems.

In this article, we concentrates on analyzing the impacts of the unknown control effectiveness challenge on the stability and robustness of the nonlinear incremental control framework and then on proposing a method to solve this challenge. The main contributions of this article are summarized as follows:

1) Derive a unified Lyapunov-based stability proof for MIMO nonlinear perturbed systems utilizing nonlinear incremental control despite the perturbation compensation techniques (adaptive, disturbance observer, or sliding-mode augmentations).
2) Expose that none of the existing nonlinear incremental control methods can deal with the unknown control direction challenge because one critical stability criterion is violated.
3) Propose two Nussbaum function-based adaptive nonlinear incremental control methods for dynamic systems with partially known CEM (control direction is unknown) and completely unknown CEM, respectively.

The stability and robustness of proposed methods are proved theoretically and demonstrated by fault-tolerant flight control numerical simulations.

The rest of this article is structured as follows. The preliminary is given in Section II. The limitations of the existing nonlinear incremental control are exposed in Section III. Section IV proposes two Nussbaum function-based adaptive nonlinear incremental control methods for MIMO systems. Finally, the numerical simulation and results is delivered in Section V. Section VI concludes this article.

Notations: $\mathbb{R}^n$ is the n-dimensional real space and $\mathbb{R}^{n\times m}$ is the set of real $n \times m$ matrices. $\text{sgn}(\boldsymbol{x}) = \text{diag}(\text{sign}(x_i)) \in \mathbb{R}^{n\times n}$ $(i = 1, 2, \ldots, n)$ for a vector $\boldsymbol{x} \in \mathbb{R}^n$. $\|\boldsymbol{x}\|$ represents the Euclidean norm of $\boldsymbol{x}$. $|\boldsymbol{x}| = [|x_1|, |x_2|, \ldots, |x_n|]^\mathsf{T}$ represents the absolute vector of $\boldsymbol{x} \in \mathbb{R}^n$. $\boldsymbol{f}(\boldsymbol{x})|_0$ indicates the value of $\boldsymbol{f}(\boldsymbol{x})$ at the previous time step $\boldsymbol{x} = \boldsymbol{x}(t - h)$, where h represents one sampling time step. $\boldsymbol{f}(\boldsymbol{x})|_m$ means the value of $\boldsymbol{f}(\boldsymbol{x})$ at $\boldsymbol{x}_m \in [\boldsymbol{x}(t - h), \boldsymbol{x}(t)]$. $\lambda_{\max}(\boldsymbol{X})$ denotes the maximum eigenvalue of the matrix $\boldsymbol{X}$.

II. PRELIMINARY

Consider the following MIMO nonlinear control-affine system:

$$\dot{\boldsymbol{x}} = \boldsymbol{f}(\boldsymbol{x}) + \boldsymbol{G}(\boldsymbol{x})\boldsymbol{u}, \quad \boldsymbol{y} = \boldsymbol{h}(\boldsymbol{x}) \tag{1}$$

where $\boldsymbol{x} \in \mathbb{R}^n$, $\boldsymbol{y} \in \mathbb{R}^m$, and $\boldsymbol{u} \in \mathbb{R}^m$ refer to the system's state, output, and input vectors. In this article, $\boldsymbol{f} : \mathbb{R}^n \to \mathbb{R}^n$, $\boldsymbol{h} : \mathbb{R}^n \to \mathbb{R}^m$, and $\boldsymbol{G} : \mathbb{R}^n \to \mathbb{R}^{n\times m}$ are continuous functions. The corresponding input–output mapping is

$$\boldsymbol{y}^{(\boldsymbol{\rho})} = \boldsymbol{\alpha}(\boldsymbol{x}) + \boldsymbol{\mathcal{B}}(\boldsymbol{x})\boldsymbol{u} \tag{2}$$

where $\boldsymbol{\rho} = [\rho_1, \rho_2, \ldots, \rho_m]^\mathsf{T}$ is the relative degree vector; $\boldsymbol{\alpha}(\boldsymbol{x}) = [\mathcal{L}_f^{\rho_1} h_1, \mathcal{L}_f^{\rho_2} h_2, \ldots, \mathcal{L}_f^{\rho_m} h_m]^\mathsf{T}$, $\boldsymbol{\mathcal{B}}(\boldsymbol{x}) \in \mathbb{R}^{m\times m}$ and $\mathcal{B}_{ij} = \mathcal{L}_{g_j}\mathcal{L}_f^{\rho_i - 1} h_i$, where $\mathcal{L}_f^{\rho_i} h_i$ and $\mathcal{L}_{g_j}\mathcal{L}_f^{\rho_i - 1} h_i$ are the corresponding Lie derivatives.

Define the external and internal vectors as $\boldsymbol{\xi}$ and $\boldsymbol{\eta}$, respectively. The canonical form of (1) is derived by a coordinates change: $\boldsymbol{z} = [\boldsymbol{\eta}^\mathsf{T}, \boldsymbol{\xi}^\mathsf{T}]^\mathsf{T} \mapsto T(\boldsymbol{x})$ [29], which generalizes

$$\begin{cases} \dot{\boldsymbol{\eta}} = \boldsymbol{f}_{\text{in}}(\boldsymbol{\eta}, \boldsymbol{\xi}) \\ \dot{\boldsymbol{\xi}} = \boldsymbol{A}_c\boldsymbol{\xi} + \boldsymbol{B}_c[\boldsymbol{\alpha}(\boldsymbol{x}) + \boldsymbol{\mathcal{B}}(\boldsymbol{x})\boldsymbol{u}] \\ \boldsymbol{y} = \boldsymbol{C}_c\boldsymbol{\xi} \end{cases} \tag{3}$$

Applying the first-order Taylor series expansion of (2) at $t - h$ with $\boldsymbol{x}_0 = \boldsymbol{x}(t - h)$, $\boldsymbol{u}_0 = \boldsymbol{u}(t - h)$. It can be obtained that

$$\begin{aligned} \boldsymbol{y}^{(\boldsymbol{\rho})} &= \boldsymbol{y}^{(\boldsymbol{\rho})}\Big|_0 + \frac{\partial[\boldsymbol{\alpha}(\boldsymbol{x}) + \boldsymbol{\mathcal{B}}(\boldsymbol{x})\boldsymbol{u}]}{\partial \boldsymbol{x}}\Big|_0 \Delta\boldsymbol{x} \\ &\quad + \boldsymbol{\mathcal{B}}(\boldsymbol{x})\Big|_0 \Delta\boldsymbol{u} + \boldsymbol{R}_1(\boldsymbol{x}, \boldsymbol{u}, h) \\ &\triangleq \boldsymbol{y}_0^{(\boldsymbol{\rho})} + \mathcal{A}_0(\boldsymbol{x})\Delta\boldsymbol{x} + \boldsymbol{\mathcal{B}}_0(\boldsymbol{x})\Delta\boldsymbol{u} + \boldsymbol{R}_1(\boldsymbol{x}, \boldsymbol{u}, h) \end{aligned} \tag{4}$$

where $\boldsymbol{R}_1$ represents the expansion remainder, $\Delta\boldsymbol{x}$ is the state increment in one sampling time step, and $\Delta\boldsymbol{u}$ is the control increment in one sampling step.

ASSUMPTION 1 The CEM $\boldsymbol{\mathcal{B}}_0(\boldsymbol{x})$ is continuous and $\det(\boldsymbol{\mathcal{B}}_0(\boldsymbol{x})) \neq 0$.

The control problem to be addressed is: given the system in (1) and Assumption 1, design a control law $\boldsymbol{u}(t)$ such that the output $\boldsymbol{y}$ tracks $\boldsymbol{y}_r = [y_{r,1}, y_{r,2}, \ldots, y_{r,m}]^{\mathsf{T}}$. To proceed, denote the reference vector as $\boldsymbol{r} = [\boldsymbol{r}_1, \boldsymbol{r}_2, \ldots, \boldsymbol{r}_m]^{\mathsf{T}}$ with $\boldsymbol{r}_i = [y_{r,i}, y_{r,i}^{(1)}, \ldots, y_{r,i}^{(\rho_i-1)}]$, $i = 1, \ldots, m$, and let $\boldsymbol{e} = \boldsymbol{\xi} - \boldsymbol{r}$ be the tracking error vector. Substitute (4) into (3), then the error dynamics are given by

$$\begin{aligned}\dot{\boldsymbol{e}} = {} & \boldsymbol{A}_c\boldsymbol{e} + \boldsymbol{B}_c(\boldsymbol{y}_0^{(\boldsymbol{\rho})} + \boldsymbol{\mathcal{B}}_0(\boldsymbol{x})\Delta\boldsymbol{u} - \boldsymbol{y}_r^{(\boldsymbol{\rho})}) \\ & + \boldsymbol{B}_c(\mathcal{A}_0(\boldsymbol{x})\Delta\boldsymbol{x} + \boldsymbol{R}_1(\boldsymbol{x}, \boldsymbol{u}, h))\end{aligned} \tag{5}$$

where $\boldsymbol{y}_r^{(\boldsymbol{\rho})} = [y_{r,1}^{\rho_1}, y_{r,2}^{\rho_2}, \ldots, y_{r,m}^{\rho_m}]^{\mathsf{T}}$.

A. Derivation of the INDI Control

Incremental nonlinear dynamic inversion (INDI) is the most notable nonlinear incremental control method, as proposed in [5], [6], and [10]

$$\Delta\boldsymbol{u}_{\text{indi}} = \hat{\boldsymbol{\mathcal{B}}}_0^{-1}(\boldsymbol{x})\left(\boldsymbol{v}_c - \hat{\boldsymbol{y}}_0^{(\boldsymbol{\rho})}\right), \quad \boldsymbol{u} = \boldsymbol{u}_0 + \Delta\boldsymbol{u}_{\text{indi}} \tag{6}$$

where $\hat{\boldsymbol{\mathcal{B}}}_0(\boldsymbol{x})$ denotes the estimate of CEM $\boldsymbol{\mathcal{B}}_0(\boldsymbol{x})$; $\hat{\boldsymbol{y}}_0^{(\boldsymbol{\rho})}(t)$ is the measured signal or estimate of $\boldsymbol{y}_0^{(\boldsymbol{\rho})}(t)$. The term $\boldsymbol{v}_c = -\boldsymbol{K}\boldsymbol{e} + \boldsymbol{y}_r^{(\boldsymbol{\rho})}$ denotes the INDI virtual control.

With the INDI control designed in (6), the error dynamics in (5) is governed by

$$\begin{aligned}\dot{\boldsymbol{e}} = {} & (\boldsymbol{A}_c - \boldsymbol{B}_c\boldsymbol{K})\boldsymbol{e} \\ & + \boldsymbol{B}_c[(\boldsymbol{\mathcal{B}}_0(\boldsymbol{x}) - \hat{\boldsymbol{\mathcal{B}}}_0(\boldsymbol{x}))\Delta\boldsymbol{u}_{\text{indi}} + \tilde{\boldsymbol{y}}_0^{(\boldsymbol{\rho})} + \boldsymbol{\delta}(\boldsymbol{z}, h)] \\ \triangleq {} & (\boldsymbol{A}_c - \boldsymbol{B}_c\boldsymbol{K})\boldsymbol{e} + \boldsymbol{B}_c\boldsymbol{\Delta}_{\text{indi}}\end{aligned} \tag{7}$$

with $\tilde{\boldsymbol{y}}_0^{(\boldsymbol{\rho})} = \boldsymbol{y}_0^{(\boldsymbol{\rho})} - \hat{\boldsymbol{y}}_0^{(\boldsymbol{\rho})}$ and

$$\boldsymbol{\delta}(\boldsymbol{z}, h) = [\mathcal{A}_0(\boldsymbol{x})\Delta\boldsymbol{x} + \boldsymbol{R}_1(\boldsymbol{x}, \boldsymbol{u}, h)]\Big|_{\boldsymbol{z}=T(\boldsymbol{x}_0), \boldsymbol{u}=\boldsymbol{u}_0+\Delta\boldsymbol{u}_{\text{indi}}}$$

ASSUMPTION 2 [5], [10] The measurement/estimation error of $\boldsymbol{y}_0^{(\boldsymbol{\rho})}$ is bounded; i.e., $\|\tilde{\boldsymbol{y}}_0^{(\boldsymbol{\rho})}\| \leq \bar{\delta}_y$.

REMARK 1 The sensing error $\tilde{\boldsymbol{y}}_0^{(\boldsymbol{\rho})}$, caused by noise, sensor dynamics, and sensing bias, is typically bounded [30]. When the signal $\hat{\boldsymbol{y}}_0^{(\boldsymbol{\rho})}$ is generated by an estimator or a filter, the boundedness of the estimation error is a design requirement [12], [31].

The following lemmas have been proved.

LEMMA 1 [29] If the estimated CEM satisfies $\|\boldsymbol{\mathcal{B}}_0(\boldsymbol{x})\hat{\boldsymbol{\mathcal{B}}}_0^{-1}(\boldsymbol{x}) - \boldsymbol{I}\| < 1$ and if $\boldsymbol{\delta}(\boldsymbol{z}, h)$ in (7) is bounded, then under Assumption 2, for sufficiently high sampling frequency, the perturbation term $\boldsymbol{\Delta}_{\text{indi}}$ in (7) is bounded.

LEMMA 2 [29] Given a controller that results in the error dynamics in (7), if $\|\boldsymbol{\Delta}_{\text{indi}}\| \leq \delta_\varepsilon$ is satisfied for all $\boldsymbol{z} \in \mathbb{R}^n$, and if the origin of $\dot{\boldsymbol{\eta}} = \boldsymbol{f}_{\text{in}}(\boldsymbol{\eta}, \boldsymbol{0})$ is globally exponentially stable, then this controller guarantees that the state $\boldsymbol{z}$ in (3) is globally ultimately bounded.

B. Perturbation Compensations for the INDI Control

As shown in (7), the perturbation term $\boldsymbol{\Delta}_{\text{indi}}(\boldsymbol{x}, \boldsymbol{u}, h)$ is influencing the stability and performance of the INDI control. To compensate for this term, researchers have proposed adaptive control, sliding mode control, and observer-based control augmentations for INDI to provide an online approximation of $\boldsymbol{\Delta}_{\text{indi}}(\boldsymbol{x}, \boldsymbol{u}, h)$ over a compact set $\boldsymbol{x}, \boldsymbol{u} \in \mathcal{D}$. With these augmentations, the incremental control law becomes [5], [6], [10], [11]

$$\Delta\boldsymbol{u}_{\text{indi}} = \hat{\boldsymbol{\mathcal{B}}}_0^{-1}(\boldsymbol{x})\left(\boldsymbol{v}_c + \boldsymbol{v}_n - \hat{\boldsymbol{y}}_0^{(\boldsymbol{\rho})}\right). \tag{8}$$

The nonlinear term $\boldsymbol{v}_n$ is designed for perturbation compensation, which can be an adaptive control term, an observer-based robustify term or a sliding mode control term. The typical design approaches are summarized as follows.

1) Adaptive Control [11]

$$\boldsymbol{v}_{\text{n-ad}} = -\hat{\boldsymbol{K}}_x^{\mathsf{T}}\boldsymbol{x} - \hat{\boldsymbol{\Theta}}^{\mathsf{T}}\boldsymbol{\Psi}(\boldsymbol{x}, \boldsymbol{u}, h) \tag{9}$$

where $\boldsymbol{K}_x \in \mathbb{R}^{n\times m}$ is a linear adaptive gain matrix; $\hat{\boldsymbol{\Theta}} \in \mathbb{R}^{N\times m}$ is the estimation vector of N unknown parameters; $\boldsymbol{\Psi}(\boldsymbol{x}, \boldsymbol{u}, h) = [\psi_1(\boldsymbol{x}, \boldsymbol{u}, h), \psi_2(\boldsymbol{x}, \boldsymbol{u}, h), \ldots, \psi_N(\boldsymbol{x}, \boldsymbol{u}, h)]^{\mathsf{T}} \in \mathbb{R}^N$ is the regression function vector.

2) Observer-based control

$$\boldsymbol{v}_{\text{n-obv}} = -\hat{\boldsymbol{\Delta}}_{\text{indi}} \tag{10}$$

with

$$\begin{aligned}\dot{\hat{\boldsymbol{e}}} &= (\boldsymbol{A}_c - \boldsymbol{B}_c\boldsymbol{K})\hat{\boldsymbol{e}} - \boldsymbol{L}(\boldsymbol{e} - \hat{\boldsymbol{e}}) + \boldsymbol{B}_c(\boldsymbol{v}_n + \hat{\boldsymbol{\Delta}}_{\text{indi}}) \\ \hat{\boldsymbol{\Delta}}_{\text{indi}} &= -\boldsymbol{\Gamma}_1(\boldsymbol{e} - \hat{\boldsymbol{e}}) - \int_0^t \boldsymbol{\Gamma}_2(\boldsymbol{e} - \hat{\boldsymbol{e}})\mathrm{d}\tau\end{aligned} \tag{11}$$

where the matrix $\boldsymbol{L} \in \mathbb{R}^{n\times n}$ is selected to be Hurwitz; $\boldsymbol{\Gamma}_1, \boldsymbol{\Gamma}_2 \in \mathbb{R}^{m\times n}$ are the time-varying parameters to be designed (see [32]); $\hat{\boldsymbol{\Delta}}_{\text{indi}}$ denotes the estimate of $\boldsymbol{\Delta}_{\text{indi}}$.

3) Sliding-mode control

$$\begin{aligned}\boldsymbol{v}_{\text{n-smc}} &= -\boldsymbol{K}_s\text{sgn}(\boldsymbol{\sigma})^{\boldsymbol{\gamma}} \\ &= -[K_{s,1}|\sigma_1|^{\gamma_1}\text{sign}(\sigma_1), \ldots, K_{s,m}|\sigma_m|^{\gamma_m}\text{sign}(\sigma_m)]^{\mathsf{T}}\end{aligned} \tag{12}$$

with

$$\boldsymbol{\sigma} = \boldsymbol{S}\boldsymbol{e} - \boldsymbol{S}\boldsymbol{e}(0) + \int_0^t \boldsymbol{K}_o\boldsymbol{e}\mathrm{d}\tau \tag{13}$$

where $0 < \gamma_i < 1$, $\boldsymbol{K}_o = -\boldsymbol{S}(\boldsymbol{A}_c - \boldsymbol{B}_c\boldsymbol{K})$, $\boldsymbol{S} = \text{diag}\{\boldsymbol{S}_i\}$ with $\boldsymbol{S}_i = [K_{i,1}, K_{i,\rho_i-1}, 1]$.

The involvement of $\boldsymbol{v}_n$ updates the closed-loop system dynamics in (7) into

$$\dot{\boldsymbol{e}} = (\boldsymbol{A}_c - \boldsymbol{B}_c\boldsymbol{K})\boldsymbol{e} + \boldsymbol{B}_c(\boldsymbol{v}_n + \boldsymbol{\Delta}_{\text{indi}}). \tag{14}$$

REMARK 2 In the literature, many control methods directly assume that the perturbation term $\boldsymbol{\Delta}_{\text{indi}}(\boldsymbol{x}, \boldsymbol{u}, h)$ is

bounded [1], [6], [11], [12]. However, because of the usage of the dynamic inversion architecture, the term $\boldsymbol{\Delta}_{\text{indi}}(\boldsymbol{x}, \boldsymbol{u}, h)$ is a function of both $\boldsymbol{x}$ and $\boldsymbol{u}$. Thus, its boundedness cannot be directly used as a precondition for the stability proof of the closed-loop system. By contrast, the $\boldsymbol{\Delta}_{\text{indi}}(\boldsymbol{x}, \boldsymbol{u}, h)$ term will be explicitly analyzed in this article without this rough assumption.

III. ANALYSIS AND LIMITATION EXPOSURE OF INDI

Although the robustness of the INDI control can be enhanced by adaptive [see (9)], observer-based [see(10)], and sliding-mode [see (12)] virtual control laws, this section will expose that none of these augmentations can relax one critical stability condition of the INDI control.

A. A Unified Stability and Robustness Proof

First, a unified Lyapunov-based stability proof for the perturbed nonlinear error dynamics using nonlinear incremental control is presented.

THEOREM 1 Under Assumptions 1 and 2, for the nonlinear system in (3), if

$$\left\| \boldsymbol{\mathcal{B}}_0(\boldsymbol{x})\hat{\boldsymbol{\mathcal{B}}}_0^{-1}(\boldsymbol{x}) - \boldsymbol{I} + \left(\frac{\partial \boldsymbol{\mathcal{B}}(\boldsymbol{x})}{\partial \boldsymbol{x}}\Big|_m \Delta \boldsymbol{x} \right) \hat{\boldsymbol{\mathcal{B}}}_0^{-1}(\boldsymbol{x}) \right\| < 1 \quad (15)$$

then using the control in (8), there exists a finite time period T such that $\|\boldsymbol{v}_n + \boldsymbol{\Delta}_{\text{indi}}(\boldsymbol{x}, \boldsymbol{u}, h)\| \le \bar{\varepsilon},\ \forall t > t(0) + T$ and the tracking error $\boldsymbol{e}$ in (14) is globally ultimately bounded by $\frac{\bar{\varepsilon}}{|\lambda_{\max}(\boldsymbol{A}_c - \boldsymbol{B}_c\boldsymbol{K})|}$. If further the origin of $\dot{\boldsymbol{\eta}} = \boldsymbol{f}_{\text{in}}(\boldsymbol{\eta}, \boldsymbol{0})$ is globally exponentially stable, then the state $\boldsymbol{z}$ in (3) is also globally ultimately bounded.

PROOF Rewrite (8) as

$$\boldsymbol{v} = \hat{\boldsymbol{\mathcal{B}}}_0(\boldsymbol{x})\Delta \boldsymbol{u}_{\text{indi}} = \boldsymbol{v}_c + \boldsymbol{v}_n - \hat{\boldsymbol{y}}_0^{(\boldsymbol{\rho})} \quad (16)$$

then the perturbation term $\boldsymbol{\Delta}_{\text{indi}}$ in (7) becomes

$$\begin{aligned} \boldsymbol{\Delta}_{\text{indi}} &= \tilde{\boldsymbol{y}}_0^{(\boldsymbol{\rho})} + (\boldsymbol{\mathcal{B}}_0(\boldsymbol{x}) - \hat{\boldsymbol{\mathcal{B}}}_0(\boldsymbol{x}))\Delta \boldsymbol{u}_{\text{indi}} \\ &\quad + \mathcal{A}_0(\boldsymbol{x})\Delta \boldsymbol{x} + \mathcal{A}_m(\boldsymbol{x})\Delta \boldsymbol{x}^2 + \mathcal{B}_m(\boldsymbol{x})\Delta \boldsymbol{x}\Delta \boldsymbol{u}_{\text{indi}} \\ &= [\boldsymbol{\mathcal{B}}_0(\boldsymbol{x})\hat{\boldsymbol{\mathcal{B}}}_0^{-1}(\boldsymbol{x}) - \boldsymbol{I} + \mathcal{B}_m(\boldsymbol{x})\Delta \boldsymbol{x}\hat{\boldsymbol{\mathcal{B}}}_0^{-1}(\boldsymbol{x})]\boldsymbol{v} \\ &\quad + \tilde{\boldsymbol{y}}_0^{(\boldsymbol{\rho})} + \mathcal{A}_0(\boldsymbol{x})\Delta \boldsymbol{x} + \mathcal{A}_m(\boldsymbol{x})\Delta \boldsymbol{x}^2 \\ &\triangleq \boldsymbol{\Phi}(\boldsymbol{x})\boldsymbol{v} + \tilde{\boldsymbol{y}}_0^{(\boldsymbol{\rho})} + \mathcal{A}_0(\boldsymbol{x})\Delta \boldsymbol{x} + \mathcal{A}_m(\boldsymbol{x})\Delta \boldsymbol{x}^2 \end{aligned} \quad (17)$$

where

$$\mathcal{A}_m(\boldsymbol{x}) = \frac{1}{2}\frac{\partial^2[\boldsymbol{\alpha}(\boldsymbol{x}) + \boldsymbol{\mathcal{B}}(\boldsymbol{x})\boldsymbol{u}]}{\partial^2 \boldsymbol{x}}\Big|_m, \quad \mathcal{B}_m(\boldsymbol{x}) = \frac{\partial \boldsymbol{\mathcal{B}}(\boldsymbol{x})}{\partial \boldsymbol{x}}\Big|_m \quad (18)$$

1) Adaptive control
The online approximation of $\boldsymbol{\Delta}_{\text{indi}}(\boldsymbol{x}, \boldsymbol{u}, h)$ in adaptive control [see (9)] often requires a matching condition:

$$\boldsymbol{v}_{\text{n-ad}}^{\star} + \boldsymbol{\Delta}_{\text{indi}}(\boldsymbol{x}, \boldsymbol{u}, h) = \boldsymbol{\varepsilon}(\boldsymbol{x}, \boldsymbol{u}, h) \quad (19)$$

where $\boldsymbol{v}_{\text{n-ad}}^{\star}$ is the adaptive control in (9) with ideal gains; $\boldsymbol{\varepsilon}(\boldsymbol{x}, \boldsymbol{u}, h)$ is a bounded neighborhood over a domain $\mathcal{D}$. To satisfy the matching condition in (19), the mapping $\boldsymbol{v}_{\text{n-ad}} \mapsto -\boldsymbol{\Delta}_{\text{indi}}$ must be a contraction [33]. This means that if $\|\frac{\partial \boldsymbol{\Delta}_{\text{indi}}}{\partial \boldsymbol{v}_n}\| < 1$ is satisfied, then a unique solution exists for $\boldsymbol{v}_{\text{n-ad}}^{\star} = -\boldsymbol{\Delta}_{\text{indi}}$ with some maximum error $\bar{\varepsilon}$. In other words, if

$$\begin{aligned} \left\| \frac{\partial \boldsymbol{\Delta}_{\text{indi}}}{\partial \boldsymbol{v}_n} \right\| &= \left\| \frac{\partial \boldsymbol{\Delta}_{\text{indi}}}{\partial \Delta \boldsymbol{u}_{\text{indi}}} \cdot \frac{\partial \Delta \boldsymbol{u}_{\text{indi}}}{\partial \boldsymbol{v}} \cdot \frac{\partial \boldsymbol{v}}{\partial \boldsymbol{v}_n} \right\| \\ &= \|\boldsymbol{\mathcal{B}}_0(\boldsymbol{x})\hat{\boldsymbol{\mathcal{B}}}_0^{-1}(\boldsymbol{x}) - \boldsymbol{I} + \mathcal{B}_m(\boldsymbol{x})\Delta \boldsymbol{x}\hat{\boldsymbol{\mathcal{B}}}_0^{-1}(\boldsymbol{x})\| < 1 \end{aligned} \quad (20)$$

then $\|\boldsymbol{v}_{\text{n-ad}} + \boldsymbol{\Delta}_{\text{indi}}\| \le \bar{\varepsilon},\ \forall t > t(0) + T$ for some finite time period T.

2) Observer-based control
By performing analogous derivations for $\boldsymbol{\Delta}_{\text{indi}}$ as in [5] and introducing the fact that $\boldsymbol{y}^{(\boldsymbol{\rho})} = \boldsymbol{v}_c + \boldsymbol{v}_n + \boldsymbol{\Delta}_{\text{indi}}$, one can write $\boldsymbol{\Delta}_{\text{indi}}$ as

$$\begin{aligned} \boldsymbol{\Delta}_{\text{indi}} = &- \boldsymbol{\Phi}(\boldsymbol{x})\boldsymbol{\Delta}_{\text{indi},0} + \boldsymbol{\Phi}(\boldsymbol{x})(\Delta \boldsymbol{v}_c + \Delta \boldsymbol{v}_n) \\ &+ (\boldsymbol{I} + \boldsymbol{\Phi}(\boldsymbol{x}))\tilde{\boldsymbol{y}}_0 + \mathcal{A}_0(\boldsymbol{x})\Delta \boldsymbol{x} + \mathcal{A}_m(\boldsymbol{x})\Delta \boldsymbol{x}^2. \end{aligned} \quad (21)$$

Since the control terms $\boldsymbol{v}_c$ and $\boldsymbol{v}_n$ are continues in time, then the corresponding incremental terms $\Delta \boldsymbol{v}_c$, $\Delta \boldsymbol{v}_n$ are in the order of magnitude of $O(h^2)$ [10], [34]. Now, assume that the $\boldsymbol{\mathcal{B}}(\boldsymbol{x})$ and $\boldsymbol{\alpha}(\boldsymbol{x})$ have bounded partial derivatives of arbitrary order with respect to $\boldsymbol{x}$, then it follows: $\lim_{h\to 0}\|\Delta \boldsymbol{v}_c\| = 0$, $\lim_{h\to 0}\|\Delta \boldsymbol{v}_n\| = 0$, $\lim_{h\to 0}\|\mathcal{A}_0(\boldsymbol{x})\Delta \boldsymbol{x} + \mathcal{A}_m(\boldsymbol{x})\Delta \boldsymbol{x}^2\| = 0$. Therefore, there exists a h such that $\|\Delta \boldsymbol{v}_c(k)\| \le \bar{\delta}_{v_c}$, $\|\Delta \boldsymbol{v}_n(k)\| \le \bar{\delta}_{v_n}$, and $\|\mathcal{A}_0(k)\Delta \boldsymbol{x}(k) + \mathcal{A}_m(k)\Delta \boldsymbol{x}^2(k)\| \le \bar{\delta}_A$. Using these properties, (21) satisfies

$$\begin{aligned} \|\boldsymbol{\Delta}_{\text{indi}}(k)\| \le &\|\boldsymbol{\Phi}(\boldsymbol{x})\|\|\boldsymbol{\Delta}_{\text{indi}}(k-1)\| + \bar{\delta}_A + \bar{\delta}_y \\ &+ \|\boldsymbol{\Phi}(\boldsymbol{x})\|\bar{\delta}_y + \|\boldsymbol{\Phi}(\boldsymbol{x})\|(\bar{\delta}_{v_c} + \bar{\delta}_{v_n}). \end{aligned} \quad (22)$$

Therefore, the term $\boldsymbol{\Delta}_{\text{indi}}$ is bounded if

$$\|\boldsymbol{\mathcal{B}}_0(\boldsymbol{x})\hat{\boldsymbol{\mathcal{B}}}_0^{-1}(\boldsymbol{x}) - \boldsymbol{I} + \mathcal{B}_m(\boldsymbol{x})\Delta \boldsymbol{x}\hat{\boldsymbol{\mathcal{B}}}_0^{-1}(\boldsymbol{x}))\| < 1. \quad (23)$$

Given a bounded $\boldsymbol{\Delta}_{\text{indi}}$, any sliding mode observer or disturbance observer can be used to estimate it with a bounded estimate error $\|\boldsymbol{\Delta}_{\text{indi}} - \hat{\boldsymbol{\Delta}}_{\text{indi}}\| \le \bar{\varepsilon},\ \forall t > t_0 + T$. By using the disturbance observer in (11) and the control law $\boldsymbol{v}_{\text{n-obv}} = -\hat{\boldsymbol{\Delta}}_{\text{indi}}$, the closed-loop dynamics yields

$$\dot{\boldsymbol{e}} = (\boldsymbol{A}_c - \boldsymbol{B}_c\boldsymbol{K})\boldsymbol{e} + \boldsymbol{B}_c(\boldsymbol{\Delta}_{\text{indi}} - \hat{\boldsymbol{\Delta}}_{\text{indi}}), \forall t > t(0) + T \quad (24)$$

and $\boldsymbol{\varepsilon}(\boldsymbol{x}, \boldsymbol{u}, h) = \boldsymbol{\Delta}_{\text{indi}} - \hat{\boldsymbol{\Delta}}_{\text{indi}}$ is the bounded estimate error with $\|\boldsymbol{\varepsilon}(\boldsymbol{x}, \boldsymbol{u}, h)\| \le \bar{\varepsilon}$.

3) Sliding mode control
Consider the candidate Lyapunov function $V = \frac{1}{2}\boldsymbol{\sigma}^T\boldsymbol{\sigma}$ for the sliding mode control augmented INDI in (12), then it follows:

$$\begin{aligned} \dot{V} &= \boldsymbol{\sigma}^T(\boldsymbol{y}^{(\boldsymbol{\rho})} - \boldsymbol{v}_c) = \boldsymbol{\sigma}^T(\boldsymbol{v}_{\text{n-smc}} + \boldsymbol{\Delta}_{\text{indi}}) \\ &\le \sum_{i=1}^{m} -K_{s,i}|\sigma_i|^{\gamma_i+1} + |\boldsymbol{\Delta}_{\text{indi,i}}||\sigma_i| \end{aligned}$$

$$\leq \sum_{i=1}^{m} -\eta_i|\sigma_i|, \quad \forall|\sigma_i| \geq \left(\frac{\eta_i + |\boldsymbol{\Delta}_{\text{indi,i}}|}{K_{s,i}}\right)^{\frac{1}{\gamma_i}} \tag{25}$$

where $\eta_i > 0$. Analogous to the analysis from (21) to (23), $|\boldsymbol{\Delta}_{\text{indi,i}}|$ is bounded if $\|\boldsymbol{\Phi}(\boldsymbol{x})\| < 1$. Thus, (25) proves that when $\|\boldsymbol{\Phi}(x)\| < 1$ is valid, then the sliding variables σ_i is ultimately bounded by $\left(\frac{\eta_i+|\boldsymbol{\Delta}_{\text{indi,i}}|}{K_{s,i}}\right)^{\frac{1}{\gamma_i}}$ in a finite time T.

The variable $\tilde{\boldsymbol{d}} = \boldsymbol{\sigma}(t), t > t(0) + T$ viewed as the sliding variable in the quasi-sliding motion, is bounded with $|\tilde{d}_i| < \bar{\delta}_{s,i} \leq \bar{\delta}_s$ and $\bar{\delta}_s = \sup_{i=1,\ldots,m}\left(\frac{\eta_i+|\boldsymbol{\Delta}_{\text{indi,i}}|}{K_{s,i}}\right)^{\frac{1}{\gamma_i}}$. On the quasi-sliding surface, the dynamics of the tracking error $\boldsymbol{e}$ becomes

$$\dot{\boldsymbol{e}} = (\boldsymbol{A}_c - \boldsymbol{B}_c\boldsymbol{K})\boldsymbol{e} + \boldsymbol{B}_c(\boldsymbol{S}\boldsymbol{B}_c)^{-1}\tilde{\boldsymbol{d}}, \ \forall t > t(0) + T \tag{26}$$

in which $\boldsymbol{\varepsilon}(\boldsymbol{x}, \boldsymbol{u}, h) = \boldsymbol{v}_{\text{n-smc}} + \boldsymbol{\Delta}_{\text{indi}} = (\boldsymbol{S}\boldsymbol{B}_c)^{-1}\tilde{\boldsymbol{d}}$ is ultimately bounded as $\|\boldsymbol{\varepsilon}(\boldsymbol{x}, \boldsymbol{u}, h)\| \leq \bar{\varepsilon}$.

By far, it is apparent that no matter which augmentation is applied for the nonlinear incremental control, the resulting error dynamics are uniformed as

$$\dot{\boldsymbol{e}} = (\boldsymbol{A}_c - \boldsymbol{B}_c\boldsymbol{K})\boldsymbol{e} + \boldsymbol{B}_c\boldsymbol{\varepsilon}(\boldsymbol{x}, \boldsymbol{u}, h), \ \forall t > t(0) + T \tag{27}$$

in which $\boldsymbol{\varepsilon}(\boldsymbol{x}, \boldsymbol{u}, h)$ represents the generalized approximation error of the perturbation term $\boldsymbol{\Delta}_{\text{indi}}(\boldsymbol{x}, \boldsymbol{u}, h)$. Since $\boldsymbol{K}$ is designed for making $\boldsymbol{A}_c - \boldsymbol{B}_c\boldsymbol{K}$ Hurwitz, then (27) also indicates that the tracking error $\boldsymbol{e}$ is ultimately bounded by $\frac{\bar{\varepsilon}}{|\lambda_{\max}(\boldsymbol{A}_c - \boldsymbol{B}_c\boldsymbol{K})|}$. Because of the boundedness of $\boldsymbol{e}$, we can guarantee the globally ultimately boundedness of the state $\boldsymbol{z}$ in (3) by directly using Lemma 2.

This completes the proof. ■

COROLLARY 1 If $\|\boldsymbol{\Phi}(\boldsymbol{x})\| \leq \bar{b} < 1$, for a sufficiently high sampling frequency h, and a bounded sensing error $\|\tilde{\boldsymbol{y}}_0^{(\boldsymbol{\rho})}\| \leq \bar{\delta}_y$, then the residual error $\boldsymbol{\Delta}_{\text{indi}}$ of INDI in (7) and the tracking error $\boldsymbol{e}$ in (14) are ultimately bounded as

$$\lim_{t\to\infty} \|\boldsymbol{\Delta}_{\text{indi}}\| \leq \frac{(\bar{\delta}_{v_c} + \bar{\delta}_{v_n})\bar{b} + \bar{\delta}_A + \bar{\delta}_y\bar{b}(1 + \bar{b})}{1 - \bar{b}} \tag{28}$$

$$\lim_{t\to\infty} \|\boldsymbol{e}\| \leq \frac{h(\bar{\delta}_{v_c} + \bar{\delta}_{v_n})\bar{b} + h\bar{\delta}_A + h\bar{\delta}_y\bar{b}(1 + \bar{b})}{(1 - \bar{b})(1 - \bar{\lambda})} \tag{29}$$

where $\|\boldsymbol{I} + h(\boldsymbol{A}_c - \boldsymbol{B}_c\boldsymbol{K})\| \leq \bar{\lambda} < 1$.

PROOF This corollary can be proved analogous to the stability analysis in the [10, Sec. II-B]. ■

REMARK 3 Theorem 1 is much more general than the stability analysis in [10] because Theorem 1 is independent of any specific perturbation compensation approaches, and the $\Delta\boldsymbol{x}$ related term is also accounted for in the (15) of Theorem 1.

REMARK 4 If the CEM $\boldsymbol{\mathcal{B}}_0(\boldsymbol{x})$ is not a square matrix, but is $\boldsymbol{\mathcal{B}}_0(\boldsymbol{x}) \in \mathbb{R}^{l\times m}$, then the right pseudoinverse can be used in (15) as long as $\boldsymbol{\mathcal{B}}_0(\boldsymbol{x})$ has full row rank. Then, the condition can be redefined as

$$\|\boldsymbol{\mathcal{B}}_0(\boldsymbol{x})\hat{\boldsymbol{\mathcal{B}}}_0^{+}(\boldsymbol{x}) - \boldsymbol{I} + \mathcal{B}_m(\boldsymbol{x})\Delta\boldsymbol{x}\hat{\boldsymbol{\mathcal{B}}}_0^{+}(\boldsymbol{x})\| < 1 \tag{30}$$

where $\hat{\boldsymbol{\mathcal{B}}}_0^{+}(\boldsymbol{x}) = \hat{\boldsymbol{\mathcal{B}}}_0^{\mathsf{T}}(\boldsymbol{x})(\hat{\boldsymbol{\mathcal{B}}}_0(\boldsymbol{x})\hat{\boldsymbol{\mathcal{B}}}_0^{\mathsf{T}}(\boldsymbol{x}))^{-1}$.

REMARK 5 Theorem 1 proves that the condition in (15) is essential for nonlinear incremental control. Theorem 1 also reveals that (15) is identical to the matching condition in dynamic inversion-based adaptive control design.

B. Stability Analysis for Unknown Control Directions

Theorem 1 has exposed that the condition in (15) is crucial for stability guarantee despite, which augmentation technique is applied. It should be underlined that the elements of the CEM may switch their signs due to aeroelastic effects, severe faulty conditions, and/or coupling effects [33]. The CEM $\boldsymbol{\mathcal{B}}(\boldsymbol{x})$ is diagonally dominant when considering aircraft attitude dynamics. It is noteworthy that the condition $\|\boldsymbol{\Phi}(\boldsymbol{x})\| < 1$ in Theorem 1 would be violated when the signs of diagonal entries of $\hat{\boldsymbol{\mathcal{B}}}(\boldsymbol{x})$ and $\boldsymbol{\mathcal{B}}(\boldsymbol{x})$ don't match. Consequently, the stability of nonlinear incremental control cannot be ensured even with the robustify augmentations.

Considering model uncertainties, actuator faults, structural damage, and unknown control direction, the CEM is expanded as $\boldsymbol{\mathcal{B}}_0(\boldsymbol{x}) = \hat{\boldsymbol{\mathcal{B}}}_0(\boldsymbol{x})\boldsymbol{\Lambda} + \Delta\boldsymbol{\mathcal{B}}_0(\boldsymbol{x})$, where $\hat{\boldsymbol{\mathcal{B}}}_0(\boldsymbol{x})$ is the nominal CEM; $\boldsymbol{\Lambda}(t) = \text{diag}\{w_1, w_2, \ldots, w_m\}$ describes the control direction with non-zero real elements; $\Delta\boldsymbol{\mathcal{B}}_0(\boldsymbol{x})$ represents the CEM uncertainties. Consequently, (4) is rewritten as

$$\begin{aligned}\boldsymbol{y}^{(\boldsymbol{\rho})} = \boldsymbol{y}_0^{(\boldsymbol{\rho})} &+ (\hat{\boldsymbol{\mathcal{B}}}_0(\boldsymbol{x})\boldsymbol{\Lambda} + \Delta\boldsymbol{\mathcal{B}}_0(\boldsymbol{x}))\Delta\boldsymbol{u} \\ &+ \mathcal{A}_0(\boldsymbol{x})\Delta\boldsymbol{x} + \boldsymbol{R}_1(\boldsymbol{x}, \boldsymbol{u}, h).\end{aligned} \tag{31}$$

Define $\boldsymbol{\mathcal{D}}_m(\boldsymbol{x}) = (\mathcal{B}_m(\boldsymbol{x})\Delta\boldsymbol{x} + \Delta\boldsymbol{\mathcal{B}}_0(\boldsymbol{x}))\hat{\boldsymbol{\mathcal{B}}}_0^{-1}(\boldsymbol{x})$. Model the unknown control direction matrix $\boldsymbol{\Lambda}$ as

$$\boldsymbol{\Lambda} = \boldsymbol{\Lambda}_1 + \boldsymbol{\Lambda}_2, \quad \boldsymbol{\Lambda}_1 > 0, \ \boldsymbol{\Lambda}_2 < 0. \tag{32}$$

THEOREM 2 Consider the input–output mapping in (31). If its CEM satisfies

$$\begin{cases} \|\hat{\boldsymbol{\mathcal{B}}}_0(\boldsymbol{x})|\boldsymbol{\Lambda}|\hat{\boldsymbol{\mathcal{B}}}_0^{-1}(\boldsymbol{x}) + \boldsymbol{\mathcal{D}}_m(\boldsymbol{x}) - \boldsymbol{I}\| < 1 \\ \text{tr}\left(\boldsymbol{\Lambda}_1(\hat{\boldsymbol{\mathcal{B}}}_0^{\mathsf{T}}(\boldsymbol{x})\hat{\boldsymbol{\mathcal{B}}}_0(\boldsymbol{x}))^{-1}|\boldsymbol{\Lambda}_2|\hat{\boldsymbol{\mathcal{B}}}_0^{\mathsf{T}}(\boldsymbol{x})\hat{\boldsymbol{\mathcal{B}}}_0(\boldsymbol{x})\right) \\ +\text{tr}\left(\boldsymbol{\mathcal{D}}_m^{\mathsf{T}}\hat{\boldsymbol{\mathcal{B}}}_0(\boldsymbol{x})|\boldsymbol{\Lambda}_2|\hat{\boldsymbol{\mathcal{B}}}_0^{-1}(\boldsymbol{x})\right) - \text{tr}(\boldsymbol{\Lambda}_2) < 0 \\ \|\hat{\boldsymbol{\mathcal{B}}}_0(\boldsymbol{x})|\boldsymbol{\Lambda}|\hat{\boldsymbol{\mathcal{B}}}_0^{-1}(\boldsymbol{x})\|^2 + \|\boldsymbol{\mathcal{D}}_m\|^2 - 2\text{tr}(\boldsymbol{\mathcal{D}}_m) + m \\ -2\text{tr}(\boldsymbol{\Lambda}_1) + 2\text{tr}\left(\boldsymbol{\mathcal{D}}_m^{\mathsf{T}}\hat{\boldsymbol{\mathcal{B}}}_0(\boldsymbol{x})\boldsymbol{\Lambda}_1\hat{\boldsymbol{\mathcal{B}}}_0^{-1}(\boldsymbol{x})\right) > 1 \end{cases} \tag{33}$$

where $|\boldsymbol{\Lambda}| = \text{diag}\{|w_1|, |w_2|, \ldots, |w_m|\}$, then as long as any one of the signs of w_i is incorrectly estimated, the stability criterion (15) in Theorem 1 will be broken.

PROOF For the system in (31), the stability condition (15) becomes

$$\|\hat{\boldsymbol{\mathcal{B}}}_0(\boldsymbol{x})\boldsymbol{\Lambda}\hat{\boldsymbol{\mathcal{B}}}_0^{-1}(\boldsymbol{x}) + \boldsymbol{\mathcal{D}}_m(\boldsymbol{x}) - \boldsymbol{I}\| < 1. \tag{34}$$

Denote

$$\boldsymbol{\Psi} = \hat{\boldsymbol{\mathcal{B}}}_0(\boldsymbol{x})\boldsymbol{\Lambda}\hat{\boldsymbol{\mathcal{B}}}_0^{-1}(\boldsymbol{x}) + \boldsymbol{\mathcal{D}}_m(\boldsymbol{x})$$

$$\boldsymbol{\Psi}_{|\Delta|} = \hat{\boldsymbol{\mathcal{B}}}_0(\boldsymbol{x})|\boldsymbol{\Lambda}|\hat{\boldsymbol{\mathcal{B}}}_0^{-1}(\boldsymbol{x}) + \boldsymbol{\mathcal{D}}_m(\boldsymbol{x}). \tag{35}$$

Using the fact that if $\|\boldsymbol{\Psi}_{|\Delta|} - \boldsymbol{I}\| < 1$, $\mathrm{tr}((\boldsymbol{\Psi}_{|\Delta|} - \boldsymbol{I})^{\mathsf{T}}(\boldsymbol{\Psi}_{|\Delta|} - \boldsymbol{I})) < 1$, then, if the CEM satisfies $\|\boldsymbol{\Psi}_{|\Delta|} - \boldsymbol{I}\| < 1$, it follows that:

$$\begin{aligned}
&\mathrm{tr}\left((\boldsymbol{\Psi}_{|\Delta|} - \boldsymbol{I})^{\mathsf{T}}(\boldsymbol{\Psi}_{|\Delta|} - \boldsymbol{I})\right) = \mathrm{tr}\left(\boldsymbol{\Psi}_{|\Delta|}^{\mathsf{T}}\boldsymbol{\Psi}_{|\Delta|} + 2\boldsymbol{\Psi}_{|\Delta|} + \boldsymbol{I}\right)\\
&= \|\hat{\boldsymbol{\mathcal{B}}}_0(\boldsymbol{x})\boldsymbol{\Lambda}_1\hat{\boldsymbol{\mathcal{B}}}_0^{-1}(\boldsymbol{x})\|^2 + \|\hat{\boldsymbol{\mathcal{B}}}_0(\boldsymbol{x})|\boldsymbol{\Lambda}_2|\hat{\boldsymbol{\mathcal{B}}}_0^{-1}(\boldsymbol{x})\|^2\\
&\quad + 2\mathrm{tr}\left(\boldsymbol{\Lambda}_1(\hat{\boldsymbol{\mathcal{B}}}_0^{\mathsf{T}}(\boldsymbol{x})\hat{\boldsymbol{\mathcal{B}}}_0(\boldsymbol{x}))^{-1}|\boldsymbol{\Lambda}_2|\hat{\boldsymbol{\mathcal{B}}}_0^{\mathsf{T}}(\boldsymbol{x})\hat{\boldsymbol{\mathcal{B}}}_0(\boldsymbol{x})\right)\\
&\quad + 2\mathrm{tr}\left(\boldsymbol{\mathcal{D}}_m^{\mathsf{T}}\hat{\boldsymbol{\mathcal{B}}}_0(\boldsymbol{x})\boldsymbol{\Lambda}_1\hat{\boldsymbol{\mathcal{B}}}_0^{-1}(\boldsymbol{x})\right) - 2\mathrm{tr}(\boldsymbol{\Lambda}_1 + |\boldsymbol{\Lambda}_2|) + m\\
&\quad + 2\mathrm{tr}\left(\boldsymbol{\mathcal{D}}_m^{\mathsf{T}}\hat{\boldsymbol{\mathcal{B}}}_0(\boldsymbol{x})|\boldsymbol{\Lambda}_2|\hat{\boldsymbol{\mathcal{B}}}_0^{-1}(\boldsymbol{x})\right) - 2\mathrm{tr}(\boldsymbol{\mathcal{D}}_m) + \|\boldsymbol{\mathcal{D}}_m\|^2 < 1.
\end{aligned} \tag{36}$$

Define

$$\begin{aligned}
\Psi_1 &= \|\hat{\boldsymbol{\mathcal{B}}}_0(\boldsymbol{x})\boldsymbol{\Lambda}_1\hat{\boldsymbol{\mathcal{B}}}_0^{-1}(\boldsymbol{x})\|^2\\
&\quad + \|\hat{\boldsymbol{\mathcal{B}}}_0(\boldsymbol{x})|\boldsymbol{\Lambda}_2|\hat{\boldsymbol{\mathcal{B}}}_0^{-1}(\boldsymbol{x})\|^2 + \|\boldsymbol{\mathcal{D}}_m\|^2
\end{aligned} \tag{37}$$

$$\Psi_2 = 2\mathrm{tr}\left(\boldsymbol{\mathcal{D}}_m^{\mathsf{T}}\hat{\boldsymbol{\mathcal{B}}}_0(\boldsymbol{x})\boldsymbol{\Lambda}_1\hat{\boldsymbol{\mathcal{B}}}_0^{-1}(\boldsymbol{x})\right) - 2\mathrm{tr}(\boldsymbol{\mathcal{D}}_m) \tag{38}$$

$$\begin{aligned}
\Psi_3 &= 2\mathrm{tr}\left(\boldsymbol{\Lambda}_1(\hat{\boldsymbol{\mathcal{B}}}_0^{\mathsf{T}}(\boldsymbol{x})\hat{\boldsymbol{\mathcal{B}}}_0(\boldsymbol{x}))^{-1}|\boldsymbol{\Lambda}_2|\hat{\boldsymbol{\mathcal{B}}}_0^{\mathsf{T}}(\boldsymbol{x})\hat{\boldsymbol{\mathcal{B}}}_0(\boldsymbol{x})\right)\\
&\quad + 2\mathrm{tr}\left(\boldsymbol{\mathcal{D}}_m^{\mathsf{T}}\hat{\boldsymbol{\mathcal{B}}}_0(\boldsymbol{x})|\boldsymbol{\Lambda}_2|\hat{\boldsymbol{\mathcal{B}}}_0^{-1}(\boldsymbol{x})\right).
\end{aligned} \tag{39}$$

Substituting (37)– (39) into (36) yields

$$\begin{aligned}
&\mathrm{tr}\left((\boldsymbol{\Psi}_{|\Delta|} - \boldsymbol{I})^{\mathsf{T}}(\boldsymbol{\Psi}_{|\Delta|} - \boldsymbol{I})\right)\\
&\quad = \Psi_1 + \Psi_2 + \Psi_3 - 2\mathrm{tr}(\boldsymbol{\Lambda}_1 + |\boldsymbol{\Lambda}_2|) + m < 1.
\end{aligned} \tag{40}$$

Analogously, the following can be obtained for $\boldsymbol{\Psi}$:

$$\begin{aligned}
&\mathrm{tr}\left((\boldsymbol{\Psi} - \boldsymbol{I})^{\mathsf{T}}(\boldsymbol{\Psi} - \boldsymbol{I})\right)\\
&\quad = \Psi_1 + \Psi_2 - \Psi_3 - 2\mathrm{tr}(\boldsymbol{\Lambda}_1 - |\boldsymbol{\Lambda}_2|) + m.
\end{aligned} \tag{41}$$

Consider the case that $\Psi_1 + \Psi_2 - 2\mathrm{tr}(\boldsymbol{\Lambda}_1) + m > 1$ and $\Psi_3 - 2\mathrm{tr}(\boldsymbol{\Lambda}_2) < 0$, then

$$1 - (\Psi_3 - 2\mathrm{tr}(\boldsymbol{\Lambda}_2)) < \mathrm{tr}\left((\boldsymbol{\Psi} - \boldsymbol{I})^{\mathsf{T}}(\boldsymbol{\Psi} - \boldsymbol{I})\right) \not< 1. \tag{42}$$

When the CEM satisfies (33), it can be observed that (34) and (40) are contradictory, which implies $\|\boldsymbol{\Psi} - \boldsymbol{I}\| \not< 1$. Therefore, the stability criterion on CEM in theorem 1 is violated. This completes the proof. ■

It has been proved in Theorem 2 that if the control direction is unknown, then the boundedness of the perturbation term $\boldsymbol{\Delta}_{\text{indi}}$ [see (7)] and the stability of the closed-loop system cannot be ensured no matter which robustify augmentation is used.

IV. CONTROL DESIGN FOR SYSTEM WITH UNKNOWN CONTROL EFFECTIVENESS

In control practice, partial knowledge of the CEM is normally acquirable using first principles or through identification. Even so, it is possible that for a highly nonlinear and uncertain system operating in disturbing and faulty conditions, the estimation of CEM becomes nontrivial. Therefore, this section proposes two Nussbaum function-based adaptive incremental control methods (denoted as N-INDI), for the system in (3) with partial known and completely unknown CEM, respectively.

A Nussbaum-type function $\mathcal{N}(\cdot)$ has the following properties: $\lim_{k\to\infty}\sup\frac{1}{k}\int_0^k \mathcal{N}(\boldsymbol{\zeta})\mathrm{d}\boldsymbol{\zeta} = \infty$ and $\lim_{k\to\infty}\inf\frac{1}{k}\int_0^k \mathcal{N}(\boldsymbol{\zeta})\mathrm{d}\boldsymbol{\zeta} = -\infty$. The following lemma shows some useful properties of the Nussbaum-type functions.

LEMMA 3 [27], [35] Let $\lambda_i(t) : [0, \infty) \to [\underline{\lambda}, \bar{\lambda}]$ for two constants $\underline{\lambda}$ and $\bar{\lambda}$ satisfying $\underline{\lambda}\bar{\lambda} > 0$. Let $V(t)$ and $\zeta_i(t)$ be continuously differentiable functions defined on $[0, t_f)$ with $V(t) > 0$ and $\mathcal{N}(\zeta_i)$ is a Nussbaum function (type B-L). For $\forall\, t \in [0, t_f)$, $t_f \geq 0$, if

$$V(t) < c_0 \pm \int_0^{t_f}\sum_{i=1}^{m}(\lambda_i(t)\mathcal{N}(\zeta_i(t)) + a_i)\dot{\zeta}_i(t)\mathrm{d}\tau \tag{43}$$

where c_0, a_i are constants with $a_i > 0$, then $V(t)$, $\zeta_i(t)$ and $\int_0^t\sum_{i=1}^{m}(\lambda_i(t)\mathcal{N}(\zeta_i) + a_i)\dot{\zeta}_i\mathrm{d}\tau$ are bounded on $[0, t_f)$. In particular, the statement holds for $t_f = \infty$.

The following lemma about the matrix lower-diagonal-upper (LDU) decomposition will be used in the control design.

LEMMA 4 [36] Any real matrix $\boldsymbol{X} \in \mathbb{R}^{m\times m}$ with non-zero leading principal minors can be factored as $\boldsymbol{X} = \boldsymbol{LDU}$, where $\boldsymbol{L} \in \mathbb{R}^{m\times m}$ is a symmetric positive-definite matrix, $\boldsymbol{U} \in \mathbb{R}^{m\times m}$ is a unity upper triangular matrix, and $\boldsymbol{D} \in \mathbb{R}^{m\times m}$ is a diagonal matrix.

A. Partially Known CEM

In the case of partially known CEM, $\boldsymbol{\mathcal{B}}_0(\boldsymbol{x}) = \boldsymbol{\mathcal{B}}_s\boldsymbol{\Lambda}(t) + \Delta\boldsymbol{\mathcal{B}}_0(\boldsymbol{x})$, in which $\boldsymbol{\mathcal{B}}_s$ is a known constant positive symmetric matrix; $\boldsymbol{\Lambda}(t) = \mathrm{diag}\{w_1(t), \ldots, w_m(t)\}$ is the unknown matrix with nonzero real elements; $\Delta\boldsymbol{\mathcal{B}}_0(\boldsymbol{x})$ contains the CEM uncertainties. Consequently, (4) is in the following form:

$$\begin{aligned}
\boldsymbol{y}^{(\boldsymbol{\rho})} &= \boldsymbol{y}_0^{(\boldsymbol{\rho})} + \boldsymbol{\mathcal{B}}_s\boldsymbol{\Lambda}(t)\Delta\boldsymbol{u} + \Delta\boldsymbol{\mathcal{B}}_0(\boldsymbol{x})\Delta\boldsymbol{u}\\
&\quad + \mathcal{A}_0(\boldsymbol{x})\Delta\boldsymbol{x} + \boldsymbol{R}_1(\boldsymbol{x}, \boldsymbol{u}, h).
\end{aligned} \tag{44}$$

Moreover, regarding flight control, the CEM is diagonally dominant, thus the following assumption is used.

ASSUMPTION 3 The CEM uncertainty satisfies $|\Delta\boldsymbol{\mathcal{B}}_0(\boldsymbol{x})\boldsymbol{p}| \leq |\boldsymbol{\mathcal{B}}_s\boldsymbol{\Lambda}(t)\boldsymbol{p}|$ for any arbitrary vector $\boldsymbol{p}$, where the inequality is understood element-by-element.

Design the integral-type sliding variable $\boldsymbol{\sigma}$ as identical one in (13). Using (44) and (13), the dynamics of $\boldsymbol{\sigma}$ can be written as follows:

$$\begin{aligned}
\boldsymbol{\mathcal{B}}_s^{-1}\dot{\boldsymbol{\sigma}} &= \boldsymbol{\mathcal{B}}_s^{-1}(\boldsymbol{y}_0^{(\boldsymbol{\rho})} - \boldsymbol{v}_c) + \boldsymbol{\mathcal{B}}_s^{-1}\Delta\boldsymbol{\mathcal{B}}_0\Delta\boldsymbol{u} + \boldsymbol{\Lambda}\Delta\boldsymbol{u}\\
&\quad + \boldsymbol{\mathcal{B}}_s^{-1}\mathcal{A}_0(\boldsymbol{x})\Delta\boldsymbol{x} + \boldsymbol{\mathcal{B}}_s^{-1}\boldsymbol{R}_1(\boldsymbol{x}, \boldsymbol{u}, h).
\end{aligned} \tag{45}$$

The Nussbaum function based incremental control input $\Delta\boldsymbol{u}$ is designed as

$$\begin{aligned}
\Delta\boldsymbol{u}_{\text{n-indi}} &= \mathcal{N}(\boldsymbol{\zeta})\underbrace{\left(\boldsymbol{B}_s^{-1}(\boldsymbol{v}_c - \hat{\boldsymbol{y}}_0^{(\boldsymbol{\rho})}) + \boldsymbol{v}_n\right)}_{\boldsymbol{v}_{\text{ns}}}\\
\boldsymbol{u} &= \boldsymbol{u}_0 + \Delta\boldsymbol{u}_{\text{n-indi}}
\end{aligned} \tag{46}$$

where

$$\begin{aligned}\boldsymbol{v}_c &= -\boldsymbol{K}\boldsymbol{e} + \boldsymbol{y}_r^{(\boldsymbol{\rho})},\ \boldsymbol{v}_n = -\boldsymbol{K}_s \mathrm{sgn}^{\gamma}(\boldsymbol{\sigma})\\ \mathcal{N}(\boldsymbol{\zeta}) &= \mathrm{diag}\{\mathcal{N}(\zeta_1), \mathcal{N}(\zeta_i), \ldots, \mathcal{N}(\zeta_m)\}\\ \mathcal{N}(\zeta_i) &= \sinh(\zeta_i)\cos(\frac{\pi}{2}\zeta_i), \quad \dot{\zeta}_i = \sigma_i v_{\mathrm{ns},i} \end{aligned} \tag{47}$$

THEOREM 3 Under Assumptions 1, 2, and 3, consider the dynamic system in (3) with the input–output mapping in (44) and the control law in (46)–(47), if the origin of $\dot{\boldsymbol{\eta}} = \boldsymbol{f}_{\mathrm{in}}(\boldsymbol{\eta}, \boldsymbol{0})$ is globally exponentially stable, then for any bounded initial condition, all the signals involved in the closed-loop system remain bounded all the time, and the system output tracking error $\boldsymbol{e}$ is globally ultimately bounded.

PROOF Under the control law in (46), the expression in (45) becomes

$$\begin{aligned}\boldsymbol{\mathcal{B}}_s^{-1}\dot{\boldsymbol{\sigma}} = \boldsymbol{v}_n - \left(\boldsymbol{I} - \boldsymbol{\Lambda}\mathcal{N}(\boldsymbol{\zeta})\right)\boldsymbol{v}_{ns}\\ + \boldsymbol{\mathcal{B}}_s^{-1}\Delta\boldsymbol{\mathcal{B}}_0\Delta\boldsymbol{u}_{\text{n-indi}} + \boldsymbol{\delta}_{\text{n-indi}}\end{aligned} \tag{48}$$

where $\boldsymbol{\delta}_{\text{n-indi}} = \boldsymbol{\mathcal{B}}_s^{-1}(\tilde{\boldsymbol{y}}_0^{(\boldsymbol{\rho})} + \mathcal{A}_0(\boldsymbol{x})\Delta\boldsymbol{x} + \boldsymbol{R}_1(\boldsymbol{x}, \boldsymbol{u}, h)|_{z=T(\boldsymbol{x}_0),\boldsymbol{u}=\boldsymbol{u}_0+\Delta\boldsymbol{u}_{\text{n-indi}}})$. Recall that under sufficiently high sampling frequency and Assumption 2, $\boldsymbol{\delta}_{\text{n-indi}}$ is bounded. Denote $\|\boldsymbol{\delta}_{\text{n-indi}}\| \le \varepsilon_u^{\star}$.

The candidate Lyapunov function is selected as $V_s = \boldsymbol{\sigma}^{\mathsf{T}}\boldsymbol{\mathcal{B}}_s^{-1}\boldsymbol{\sigma}$, thus

$$\begin{aligned}\dot{V}_s &= \boldsymbol{\sigma}^{\mathsf{T}}(\boldsymbol{v}_n + \boldsymbol{\delta}_{\text{n-indi}}) - \boldsymbol{\sigma}^{\mathsf{T}}(\boldsymbol{I} - (\boldsymbol{\Lambda} + \boldsymbol{\mathcal{B}}_s^{-1}\Delta\boldsymbol{\mathcal{B}}_0)\mathcal{N}(\boldsymbol{\zeta}))\boldsymbol{v}_{ns}\\ &\le \boldsymbol{\sigma}^{\mathsf{T}}\boldsymbol{v}_n + \sum_{i=1}^{m}\left(-(1-\lambda_i(t)\mathcal{N}(\zeta_i))\dot{\zeta}_i + \varepsilon_u^{\star}|\sigma_i|\right)\\ &\le \sum_{i=1}^{m}\left(-\eta_i|\sigma_i| - (1-\lambda_i(t)\mathcal{N}(\zeta_i))\dot{\zeta}_i\right)\\ \forall|\sigma_i| &\ge \left(\frac{\eta_i + \varepsilon_u^{\star}}{K_{s,i}}\right)^{\frac{1}{\gamma_i}}\end{aligned} \tag{49}$$

where $\eta_i > 0$ and $\lambda_i(t) = w_i(t) + \frac{\sum_{j=1}^{m}\sigma_j\Delta b_{ji}}{\sigma_i}$ with Δb_{ji} represents the elements of $\boldsymbol{\mathcal{B}}_s^{-1}\Delta\boldsymbol{\mathcal{B}}_0$. Under Assumption 3, $\lambda_i(t)$ is bounded in $[\underline{\lambda}, \bar{\lambda}]$.

Integrating (49) over $t \in [0, t_f]$ yields

$$\begin{aligned}V_n(t_f) &\le V_n(0) - \int_0^{t_f}\sum_{i=1}^{m}(\eta_i|\sigma_i| + (1-\lambda_i(t)\mathcal{N}(\zeta_i))\dot{\zeta}_i)\mathrm{d}\tau\\ &\le V_n(0) - \int_0^{t_f}\sum_{i=1}^{m}(-\lambda_i(t)\mathcal{N}(\zeta_i) + 1)\dot{\zeta}_i\mathrm{d}\tau\end{aligned} \tag{50}$$

According to Lemma 3, for any bounded initial condition, $V_s(t)$, $\zeta_i(t)$, and $\int_0^t\sum_{i=1}^{m}(\lambda_i\mathcal{N}(\zeta_i)+1)\dot{\zeta}_i\mathrm{d}\tau$ are bounded on $[0, t)$. Consequently, the boundedness of $\boldsymbol{v}_{\mathrm{ns}}$ and $\boldsymbol{\delta}_{\text{n-indi}}$ can easily concluded from the boundedness of $\boldsymbol{\sigma}$, $\Delta\boldsymbol{x}$, and $\boldsymbol{\zeta}$. This conclusion is also true for $t_f = +\infty$, thus $\boldsymbol{\sigma} \in \mathcal{L}_\infty$. From (50), it is obvious that $\int_0^{\infty}\eta_i|\sigma_i|\mathrm{d}\tau$ exists and $\sigma_i \in \mathcal{L}_2$. Recall the expression of $\dot{\boldsymbol{\sigma}}$ in (45), because $\boldsymbol{\sigma}, \boldsymbol{\mathcal{B}}_0(\boldsymbol{x}), \boldsymbol{\delta}_{\text{n-indi}}, \boldsymbol{v}_{\mathrm{ns}} \in \mathcal{L}_\infty$, we can conclude that $\dot{\boldsymbol{\sigma}} \in \mathcal{L}_\infty$.

According to the Barbalat's lemma, $\sigma_i \to (\frac{\eta_i + \varepsilon_u^{\star}}{K_{s,i}})^{\frac{1}{\gamma_i}}$ as $t \to \infty$. In other words, the ultimate bound of σ_i equals $\bar{\delta}_{s,i} = (\frac{\eta_i+\varepsilon_u^{\star}}{K_{s,i}})^{\frac{1}{\gamma_i}}$, whose size can be assembled arbitrarily small. Denote the sliding variable in the quasi-sliding motion as $\boldsymbol{\sigma} = \tilde{\boldsymbol{d}}$ and $\bar{\delta}_s = \sup_{i=1,\ldots,m}(\frac{\eta_i+\varepsilon_u^{\star}}{K_{s,i}})^{\frac{1}{\gamma_i}}$, then $|\tilde{d}_i| \le \bar{\delta}_s$ in some finite time T_1. Consequently, the quasi-sliding mode dynamic equation follows:

$$\dot{\boldsymbol{e}} = (\boldsymbol{A}_c - \boldsymbol{B}_c\boldsymbol{K})\boldsymbol{e} + \boldsymbol{B}_c(\boldsymbol{S}\boldsymbol{B}_c)^{-1}\tilde{\boldsymbol{d}}. \tag{51}$$

Eq. (51) shows that $\boldsymbol{e}$ eventually converges to a small bound, i.e., $\|\boldsymbol{e}\| \to \varepsilon_\star = \frac{\|\boldsymbol{B}_c(\boldsymbol{S}\boldsymbol{B}_c)^{-1}\|\bar{\delta}_s}{|\lambda_{\max}(\boldsymbol{A}_c - \boldsymbol{B}_c\boldsymbol{K})|}$ as $t \to \infty$.

Note that, $\boldsymbol{r} \in \mathcal{L}_\infty$, and $\boldsymbol{\xi} \in \mathcal{L}_\infty$. Choosing a positive definite function $V_{\mathrm{in}}(\boldsymbol{\eta})$ defined in $D_\eta = \{\boldsymbol{\eta} \in \mathbb{R}^{n-\rho}\}$ as the candidate Lyapunov function for $\dot{\boldsymbol{\eta}} = \boldsymbol{f}_{\mathrm{in}}(\boldsymbol{\eta}, \boldsymbol{\xi})$. There exists class $\mathcal{K}_\infty$ functions α_1' and α_2' such that $\alpha_1'(\|\boldsymbol{e}\|) \le \|V_{\mathrm{in}}(\boldsymbol{\eta})\| \le \alpha_2'(\|\boldsymbol{e}\|)$ because the origin $\dot{\boldsymbol{\eta}} = \boldsymbol{f}_{\mathrm{in}}(\boldsymbol{\eta}, \boldsymbol{0})$ is globally exponentially stable. Meanwhile, $V_{\mathrm{in}}(\boldsymbol{\eta})$ satisfies $\frac{\partial V_{\mathrm{in}}}{\partial\boldsymbol{\eta}}\boldsymbol{f}_{\mathrm{in}}(\boldsymbol{\eta}, \boldsymbol{0}) \le -c_3\|\boldsymbol{\eta}\|^2$, $\|\frac{\partial V_{\mathrm{in}}}{\partial\boldsymbol{\eta}}\| \le c_4\|\boldsymbol{\eta}\|$ for some positive constants c_3 and c_4. Clearly, there exists a global Lipschitz constant L such that $\|\boldsymbol{f}_{\mathrm{in}}(\boldsymbol{\eta}, \boldsymbol{\xi}) - \boldsymbol{f}_{\mathrm{in}}(\boldsymbol{\eta}, \boldsymbol{0})\| \le L(\|\boldsymbol{e}\| + \|\boldsymbol{r}\|), \forall\boldsymbol{\eta} \in \mathbb{R}^{n-\rho}$ since $\boldsymbol{f}_{\mathrm{in}}(\boldsymbol{\eta}, \boldsymbol{\xi})$ is continuously differentiable and globally Lipschitz in $(\boldsymbol{\eta}, \boldsymbol{\xi})$. Analogous to the derivations in [29], the time derivative of $V_{\mathrm{in}}(\boldsymbol{\eta})$ satisfies

$$\dot{V}_{\mathrm{in}}(\boldsymbol{\eta}) \le -c_3(1-\theta_1)\|\boldsymbol{\eta}\|^2, \quad \forall\|\boldsymbol{\eta}\| \ge \frac{c_4 L(\|\boldsymbol{e}\| + \|\boldsymbol{r}\|)}{c_3\theta_1} \tag{52}$$

with constant $\theta_1 \in (0, 1)$. Denote the initial time point as t_0, and $\mu \triangleq \frac{c_4 L}{c_3\theta_1}(\sup_{t_0+T_1\le\tau\le t}(\|\boldsymbol{e}\| + \|\boldsymbol{r}\|))$. As a consequence, there exists a class $\mathcal{KL}$ function β' such that $\forall t \ge t_0 + T_1$, it has $\|\boldsymbol{\eta}\| \le \beta'(\|\boldsymbol{\eta}(t_0+T_1)\|, t - t_0 - T_1) + \alpha_1'^{-1}(\alpha_2'(\mu))$. Therefore, $\forall t \ge t_0 + T_1 + T_2$, the internal state satisfies

$$\|\boldsymbol{\eta}\| \le \frac{\theta_2\rho_i\varepsilon_u^{\star}}{2} + \alpha_1'^{-1}\left(\alpha_2'\left(\frac{c_4\,L}{c_3\theta_1}\left(\bar{\delta}_n + \bar{r}\right)\right)\right) \tag{53}$$

for some finite $T_2 > 0$ and $\theta_2 > 0$, where $\bar{\delta}_n = \frac{\|\boldsymbol{B}_c(\boldsymbol{S}\boldsymbol{B}_c)^{-1}\|\bar{\delta}_s}{|\lambda_{\max}(\boldsymbol{A}_c - \boldsymbol{B}_c\boldsymbol{K})|}$, $\|\boldsymbol{r}\| \le \bar{r}$. Eq. (53) constructs the global ultimate bounds of $\boldsymbol{\eta}$ by a class $\mathcal{K}$ function of $\lambda_{\max}(\boldsymbol{A}_c - \boldsymbol{B}_c\boldsymbol{K})$, $\bar{\delta}_s$, $\varepsilon_u^{\star}$, and $\bar{r}$.

This completes the proof. ■

B. Completely Unknown CEM

Recall (17), the dynamics in (4) is further derived as

$$\begin{aligned}\boldsymbol{y}^{(\boldsymbol{\rho})} &= \boldsymbol{y}_0^{(\boldsymbol{\rho})} + \mathcal{A}_0(\boldsymbol{x})\Delta\boldsymbol{x} + \boldsymbol{\mathcal{B}}_0(\boldsymbol{x})\Delta\boldsymbol{u} + \boldsymbol{R}_1(\boldsymbol{x}, \boldsymbol{u}, h)\\ &= \boldsymbol{y}_0^{(\boldsymbol{\rho})} + (\boldsymbol{\mathcal{B}}_0(\boldsymbol{x}) + \mathcal{B}_m(\boldsymbol{x})\Delta\boldsymbol{x})\Delta\boldsymbol{u}\\ &\quad + \mathcal{A}_0(\boldsymbol{x})\Delta\boldsymbol{x} + \mathcal{A}_m(\boldsymbol{x})\Delta\boldsymbol{x}^2\\ &\triangleq \boldsymbol{y}_0^{(\boldsymbol{\rho})} + \boldsymbol{\mathcal{B}}_{0,m}(\boldsymbol{x})\Delta\boldsymbol{u} + \mathcal{A}_0(\boldsymbol{x})\Delta\boldsymbol{x} + \mathcal{A}_m(\boldsymbol{x})\Delta\boldsymbol{x}^2.\end{aligned} \tag{54}$$

In the case of completely unknown $\boldsymbol{\mathcal{B}}_0(\boldsymbol{x})$, using Lemma 4, $\boldsymbol{\mathcal{B}}_{0,m}(\boldsymbol{x})$ can be factored as $\boldsymbol{\mathcal{B}}_{0,m}(\boldsymbol{x}) = \boldsymbol{\mathcal{B}}_s(\boldsymbol{x})\boldsymbol{\Lambda}(t)\boldsymbol{U}(\boldsymbol{x})$, where $\boldsymbol{\mathcal{B}}_s(\boldsymbol{x})$ is an unknown time-varying positive symmetric matrix; $\boldsymbol{\Lambda}(t)$ is a time-varying diagonal matrix; $\boldsymbol{U}(\boldsymbol{x})$ is a time-varying unity upper triangular matrix. Therefore, (54) leads to

$$\begin{aligned}\boldsymbol{y}^{(\boldsymbol{\rho})} = \boldsymbol{y}_0^{(\boldsymbol{\rho})} + \boldsymbol{\mathcal{B}}_s(\boldsymbol{x})\boldsymbol{\Lambda}\Delta\boldsymbol{u} - \boldsymbol{\mathcal{B}}_s(\boldsymbol{x})\boldsymbol{\Lambda}\left(\boldsymbol{I} - \boldsymbol{U}(\boldsymbol{x})\right)\Delta\boldsymbol{u}\\ + \mathcal{A}_0(\boldsymbol{x})\Delta\boldsymbol{x} + \mathcal{A}_m(\boldsymbol{x})\Delta\boldsymbol{x}^2.\end{aligned} \tag{55}$$

Denote $\boldsymbol{\Delta u} = [\Delta u_1, \Delta u_2, \ldots, \Delta u_m]^{\mathsf{T}}$. Because $\boldsymbol{I} - \boldsymbol{U}(\boldsymbol{x})$ in (55) is a strictly upper triangular matrix, thus Δu_1 depends on $\Delta u_2, \Delta u_3, \ldots, \Delta u_m$, while Δu_2 depends on $\Delta u_3, \Delta u_4, \ldots, \Delta u_m$, and so on. Therefore, it is possible to define the control signal $\Delta \boldsymbol{u}$ as a function of $(\boldsymbol{I} - \boldsymbol{U}(\boldsymbol{x}))\Delta \boldsymbol{u}$ without the appearance of static loop [37].

From (13) and (55), the dynamics of $\boldsymbol{\sigma}$ can be written as follows:

$$\begin{aligned}\boldsymbol{\mathcal{B}}_s^{-1}(\boldsymbol{x})\dot{\boldsymbol{\sigma}} &= \boldsymbol{\mathcal{B}}_s^{-1}(\boldsymbol{x})(\boldsymbol{y}_0^{(\boldsymbol{\rho})} - \boldsymbol{v}_c) - \boldsymbol{\Lambda}\left(\boldsymbol{I} - \boldsymbol{U}(\boldsymbol{x})\right)\Delta \boldsymbol{u} \\ &\quad + \boldsymbol{\Lambda}\Delta \boldsymbol{u} + \boldsymbol{\mathcal{B}}_s^{-1}(\boldsymbol{x})\mathcal{A}_0(\boldsymbol{x})\Delta \boldsymbol{x} + \boldsymbol{\mathcal{B}}_s^{-1}(\boldsymbol{x})\mathcal{A}_m(\boldsymbol{x})\Delta \boldsymbol{x}^2 \\ &= -\frac{1}{2}\dot{\boldsymbol{\mathcal{B}}}_s^{-1}(\boldsymbol{x})\boldsymbol{\sigma} + \hat{\boldsymbol{y}}_0^{(\boldsymbol{\rho})} - \boldsymbol{v}_c + \boldsymbol{\Lambda}\Delta \boldsymbol{u} + \boldsymbol{\Delta}_u(\boldsymbol{x}, \boldsymbol{u}, h) \quad (56)\end{aligned}$$

where

$$\begin{aligned}\boldsymbol{\Delta}_u(\boldsymbol{x}, \boldsymbol{u}, h) &= (\boldsymbol{\mathcal{B}}_s^{-1}(\boldsymbol{x}) - \boldsymbol{I})(\boldsymbol{y}_0^{(\boldsymbol{\rho})} - \boldsymbol{v}_c) \\ &\quad + \tilde{\boldsymbol{y}}_0^{(\boldsymbol{\rho})} + \frac{1}{2}\dot{\boldsymbol{\mathcal{B}}}_s^{-1}(\boldsymbol{x})\boldsymbol{\sigma} + \left(\boldsymbol{I} - \boldsymbol{U}(\boldsymbol{x})\right)\Delta \boldsymbol{u} \\ &\quad + \boldsymbol{\mathcal{B}}_s^{-1}(\boldsymbol{x})\mathcal{A}_0(\boldsymbol{x})\Delta \boldsymbol{x} + \boldsymbol{\mathcal{B}}_s^{-1}(\boldsymbol{x})\mathcal{A}_m(\boldsymbol{x})\Delta \boldsymbol{x}^2. \quad (57)\end{aligned}$$

The unknown smooth nonlinear time-varying state-dependent uncertainty term $\boldsymbol{\Delta}_u(\boldsymbol{x}, \boldsymbol{u}, h) = [\Delta_{u,1}, \Delta_{u,2}, \ldots, \Delta_{u,m}]^{\mathsf{T}}$ can be approximated over a compact set $\Omega_z \in \mathbb{R}^p$ as follows:

$$\Delta_{u,i}(\boldsymbol{x}, \boldsymbol{u}, h) = \boldsymbol{W}_{u,i}^T \boldsymbol{\phi}_{u,i}(\boldsymbol{x}, \boldsymbol{u}, h) + \boldsymbol{\varepsilon}_{u,i}, \quad i = 1, 2, \ldots, m \quad (58)$$

where $\boldsymbol{W}_{u,i} \in \mathbb{R}^{q_u}$ is an unknown slowly time-varying parameter vector that satisfies $\|\boldsymbol{W}_{u,i}\| \le w_u^{\star}$; $\boldsymbol{\phi}_{u,i}(\boldsymbol{x}, \boldsymbol{u}, h) : \mathbb{R}^p \to \mathbb{R}^{q_u}$ is a set of known basis functions; $\boldsymbol{\varepsilon}_{u,i}$ is the bounded state-independent reconstruction error with $|\boldsymbol{\varepsilon}_{u,i}| \le \epsilon_i^{\star}$. From the expression of $\boldsymbol{\Delta}_u(\boldsymbol{x}, \boldsymbol{u}, h)$, the function vector $\boldsymbol{\phi}_{u,i}(\boldsymbol{x}, \boldsymbol{u}, h) = [\phi_{u,i}^1, \ldots, \phi_{u,i}^j, \ldots, \phi_{u,i}^{q_u}]^{\mathsf{T}}$, $i = 1, \ldots, m$, $j = 1, \ldots, q_u$ can be determined using the Gaussian function in the following form:

$$\phi_{u,i}^j = \exp\left(-\frac{(\bar{\boldsymbol{x}}_i - \boldsymbol{\mu}_j)^{\mathsf{T}}(\bar{\boldsymbol{x}}_i - \boldsymbol{\mu}_j)}{\zeta_j^2}\right) \quad (59)$$

where $\boldsymbol{\mu}_j$ and ζ_j are the center and the width of the basis function $\phi_{u,i}(\boldsymbol{x}, \boldsymbol{u}, h)$, respectively. By carefully examining the expressions of $\Delta_{u,i}(\boldsymbol{x}, \boldsymbol{u}, h)$, we can choose $\bar{\boldsymbol{x}}_i^{\mathsf{T}} = [\boldsymbol{x}^{\mathsf{T}}, \boldsymbol{\sigma}^{\mathsf{T}}, (\boldsymbol{y}_0^{(\boldsymbol{\rho})})^{\mathsf{T}}, \boldsymbol{v}_c^{\mathsf{T}}, \Delta \boldsymbol{x}^{\mathsf{T}}, \Delta u_{i+1}, \ldots, \Delta u_m]$ for $i = 1, \ldots, m-1$. When $i = m, \bar{\boldsymbol{x}}_m^{\mathsf{T}} = [\boldsymbol{x}^{\mathsf{T}}, \boldsymbol{\sigma}^{\mathsf{T}}, (\boldsymbol{y}_0^{(\boldsymbol{\rho})})^{\mathsf{T}}, \boldsymbol{v}_c^{\mathsf{T}}, \Delta \boldsymbol{x}^{\mathsf{T}}]$.

The Nussbaum function-based adaptive incremental control input $\Delta \boldsymbol{u}(t)$ is designed as

$$\begin{aligned}\Delta \boldsymbol{u}_{\text{n-indi}} &= \mathcal{N}(\boldsymbol{\zeta})\underbrace{\left(-\hat{\boldsymbol{y}}_0^{(\boldsymbol{\rho})} + \boldsymbol{v}_c + \boldsymbol{v}_n - \hat{\boldsymbol{W}}_u^T \boldsymbol{\phi}_u(\boldsymbol{x}, \boldsymbol{u}, h)\right)}_{\boldsymbol{v}_{\text{ns}}} \\ \boldsymbol{u} &= \boldsymbol{u}_0 + \Delta \boldsymbol{u}_{\text{n-indi}} \quad (60)\end{aligned}$$

where $\mathcal{N}(\boldsymbol{\zeta})$, $\boldsymbol{v}_c$, $\boldsymbol{v}_n$ are identical to those in (47), and

$$\begin{aligned}\dot{\hat{W}}_{u,i}^j &= \mu_i^j \boldsymbol{\phi}_{u,i}^j(\boldsymbol{x}, \boldsymbol{u}, h)\sigma_i - \rho_i^j \hat{W}_{u,i}^j \sigma_i, \ \rho_i^j < \bar{\rho}_i, \\ &\quad i = 1, \ldots, m, \quad j = 1, \ldots, q_u. \quad (61)\end{aligned}$$

THEOREM 4 Under Assumptions 1 and 2, consider the dynamic system in (3) with the input–output mapping in (54) and the control law in (60) and (61), if the origin of $\dot{\boldsymbol{\eta}} = \boldsymbol{f}_{\text{in}}(\boldsymbol{\eta}, \boldsymbol{0})$ is globally exponentially stable, then for any bounded initial condition, all the signals of the closed-loop system (including $\boldsymbol{x}, \boldsymbol{u}, \boldsymbol{W}_{u,i}$) remain bounded all the time. The tracking error satisfies $\|\boldsymbol{e}\| \le \frac{\|\boldsymbol{B}_c(\boldsymbol{S}\boldsymbol{B}_c)^{-1}\|\bar{\delta}_s}{|\lambda_{\max}(\boldsymbol{A}_c - \boldsymbol{B}_c\boldsymbol{K})|}$ as $t \to \infty$, where $\bar{\delta}_s = \sup_{i=1,\ldots,m}(\frac{\bar{\rho}_i w_u^{\star}}{2K_{s,i}})^{\frac{1}{\gamma_i}}$.

PROOF Using the control law in (60) and denote $\tilde{\boldsymbol{W}}_{u,i} = \hat{\boldsymbol{W}}_{u,i} - \boldsymbol{W}_{u,i}$, the expression in (56) becomes

$$\begin{aligned}\boldsymbol{\mathcal{B}}_s^{-1}(\boldsymbol{x})\dot{\boldsymbol{\sigma}} = &-\frac{1}{2}\dot{\boldsymbol{\mathcal{B}}}_s^{-1}(\boldsymbol{x})\boldsymbol{\sigma} - \boldsymbol{K}_s \text{sgn}(\boldsymbol{\sigma})^{\boldsymbol{\gamma}} \\ &- \tilde{\boldsymbol{W}}_u^T \boldsymbol{\phi}_u(\boldsymbol{x}, \boldsymbol{u}, h) + \boldsymbol{\varepsilon}_u - \left(1 - \boldsymbol{\Lambda}\mathcal{N}(\boldsymbol{\zeta})\right)\boldsymbol{v}_{\text{ns}}. \quad (62)\end{aligned}$$

Multiplying both sides of (62) with $\boldsymbol{\sigma}^{\mathsf{T}}$ yields

$$\begin{aligned}\boldsymbol{\sigma}^{\mathsf{T}}\boldsymbol{\mathcal{B}}_s^{-1}(\boldsymbol{x})\dot{\boldsymbol{\sigma}} &= -\frac{1}{2}\boldsymbol{\sigma}^{\mathsf{T}}\dot{\boldsymbol{\mathcal{B}}}_s^{-1}(\boldsymbol{x})\boldsymbol{\sigma} - (1 - w_i\mathcal{N}(\zeta_i))\dot{\zeta}_i) \\ &+ \sum_{i=1}^m(-K_{s,i}|\sigma_i|^{\gamma_i+1} - \sigma_i\tilde{\boldsymbol{W}}_{u,i}^T\boldsymbol{\phi}_{u,i}(\boldsymbol{x}, \boldsymbol{u}, h) + \sigma_i\boldsymbol{\varepsilon}_{u,i}. \quad (63)\end{aligned}$$

The candidate Lyapunov function is selected as

$$V_n = \frac{1}{2}\boldsymbol{\sigma}^{\mathsf{T}}\boldsymbol{\mathcal{B}}_s^{-1}(\boldsymbol{x})\boldsymbol{\sigma} + \frac{1}{2}\sum_{i=1}^m \frac{1}{\boldsymbol{\mu}_i}\tilde{\boldsymbol{W}}_{u,i}^T\tilde{\boldsymbol{W}}_{u,i} \quad (64)$$

whose time derivative is derived as

$$\dot{V}_n = \boldsymbol{\sigma}^{\mathsf{T}}\boldsymbol{\mathcal{B}}_s^{-1}(\boldsymbol{x})\dot{\boldsymbol{\sigma}} + \frac{1}{2}\boldsymbol{\sigma}^{\mathsf{T}}\dot{\boldsymbol{\mathcal{B}}}_s^{-1}(\boldsymbol{x})\boldsymbol{\sigma} + \sum_{i=1}^m \frac{1}{\boldsymbol{\mu}_i}\tilde{\boldsymbol{W}}_{u,i}^T\dot{\tilde{\boldsymbol{W}}}_{u,i}. \quad (65)$$

Substituting (63) and (61) into (65), we obtain

$$\begin{aligned}\dot{V}_n = &\sum_{i=1}^m(-K_{s,i}|\sigma_i|^{\gamma_i+1} - (1 - w_i\mathcal{N}(\zeta_i))\dot{\zeta}_i) \\ &+ \sum_{i=1}^m\left(-\sigma_i\tilde{\boldsymbol{W}}_{u,i}^T\boldsymbol{\phi}_{u,i}(\boldsymbol{x}, \boldsymbol{u}, h) + \sigma_i\boldsymbol{\varepsilon}_{u,i}\right) \\ &+ \sum_{i=1}^m\left(\sigma_i\tilde{\boldsymbol{W}}_{u,i}^T\boldsymbol{\phi}_{u,i}(\boldsymbol{x}, \boldsymbol{u}, h) - \boldsymbol{\rho}_i\hat{\boldsymbol{W}}_{u,i}\sigma_i\right) \\ \le &\sum_{i=1}^m\left(-K_{s,i}|\sigma_i|^{\gamma_i+1} - (1 - w_i\mathcal{N}(\zeta_i))\dot{\zeta}_i\right) \\ &+ \sum_{i=1}^m\left(-\|\frac{\boldsymbol{\rho}_i}{2}\tilde{\boldsymbol{W}}_{u,i}\|^2 + \|\frac{\boldsymbol{\rho}_i}{2}\boldsymbol{W}_{u,i}\|^2\right) \\ \le &\sum_{i=1}^m\left(-\eta_i|\sigma_i| - (1 - w_i\mathcal{N}(\zeta_i))\dot{\zeta}_i\right) \\ \forall|\sigma_i| \ge &\left(\frac{\eta_i + \frac{\bar{\rho}_i}{2}w_u^{\star}}{K_{s,i}}\right)^{\frac{1}{\gamma_i}}. \quad (66)\end{aligned}$$

Integrating (66) over $t \in [0, t_f]$ leads to

$$V_n(t_f) \le V_n(0) - \int_0^{t_f}\sum_{i=1}^m(-w_i\mathcal{N}(\zeta_i) + 1)\dot{\zeta}_i \mathrm{d}\tau,$$

$$\forall|\sigma_i| \geq \left(\frac{\bar{\rho}_i w_u^\star}{2K_{s,i}}\right)^{\frac{1}{\gamma_i}}. \tag{67}$$

According to Lemma 3, for any bounded initial condition, $V_n(t)$, $\zeta_i(t)$, and $\int_0^t \sum_{i=1}^m (\lambda_i \mathcal{N}(\zeta_i)+1)\dot{\zeta}_i \mathrm{d}\tau$ are bounded on $[0, t)$. Consequently, the boundedness of $\boldsymbol{W}_u$ and $\boldsymbol{v}$ can be easily concluded from the boundedness of $\boldsymbol{\sigma}, \tilde{\boldsymbol{W}}_u$, and $\boldsymbol{\zeta}$. This conclusion also holds for $t_f = +\infty$, thus both $\boldsymbol{\sigma}$ and $\tilde{\boldsymbol{W}}_u \in \mathcal{L}_\infty$. From (67), it is apparent that $\int_0^\infty \eta_i|\sigma_i|\mathrm{d}\tau$ exists and $\sigma_i \in \mathcal{L}_2$. Recall the expression of $\dot{\boldsymbol{\sigma}}$ in (62), because $\boldsymbol{\sigma}, \boldsymbol{\mathcal{B}}_s^{-1}(\boldsymbol{x}), \tilde{\boldsymbol{W}}_u, \boldsymbol{\varepsilon}_u, \boldsymbol{v} \in \mathcal{L}_\infty$, and $\dot{\boldsymbol{\mathcal{B}}}_s^{-1}(\boldsymbol{x})$ is a continuous function, we can conclude that $\dot{\boldsymbol{\sigma}} \in \mathcal{L}_\infty$. According to the Barbalat's lemma, $\sigma_i \to (\frac{\eta_i + \frac{\bar{\rho}_i}{2} w_u^\star}{K_{s,i}})^{\frac{1}{\gamma_i}}$ as $t \to \infty$. In other words, the ultimate bound of σ_i equals $\bar{\delta}_{s,i} = (\frac{\eta_i + \frac{\bar{\rho}_i}{2} w_u^\star}{K_{s,i}})^{\frac{1}{\gamma_i}}$, $i = 1, \ldots, m$, whose size can be made arbitrarily small.

Analogous to the proof in Theorem 3, denote $\tilde{\boldsymbol{d}} = \boldsymbol{\sigma}(t), t > t(0) + T_1$, and $\bar{\delta}_s = \sup_{i=1,\ldots,m}(\frac{\eta_i + \frac{\bar{\rho}_i}{2} w_u^\star}{K_{s,i}})^{\frac{1}{\gamma_i}}$, then $|\tilde{d}_i| \leq \bar{\delta}_s$ in some finite time T_1. Let $\bar{r}$ be the upper bound of $\|\boldsymbol{r}\|$. We can also obtain that the internal state satisfies

$$\|\boldsymbol{\eta}\| \leq \frac{\theta_2 \rho_i w_u^\star}{2} + \alpha_1'^{-1}\left(\alpha_2'\left(\frac{c_4 L}{c_3 \theta_1}\left(\bar{\delta}_n + \bar{r}\right)\right)\right). \tag{68}$$

$\forall t \geq t_0 + T_1 + T_2$, where $T_2 > 0$ represents some finite time period; $\theta_2 > 0$; $\bar{\delta}_n = \frac{\|\boldsymbol{B}_c(\boldsymbol{S}\boldsymbol{B}_c)^{-1}\|\bar{\delta}_s}{|\lambda_{\max}(\boldsymbol{A}_c - \boldsymbol{B}_c\boldsymbol{K})|}$. This shows that a class $\mathcal{K}$ function of $\lambda_{\max}(\boldsymbol{A}_c - \boldsymbol{B}_c\boldsymbol{K})$, $w_u^\star$, $\bar{\delta}_s$, and $\bar{r}$ bounds $\boldsymbol{\eta}$ globally and ultimately. ■

Although in [10], a control-direction-based discrete-time incremental sliding mode control is proposed to deal with control reversal, the control direction is assumed to be reversed but known. By contrast, the newly proposed Nussbaum function-based adaptive incremental control in this article has completely solved the control challenge of system with unknown control direction. The Nussbaum function identifies the control direction online while the adaptive control algorithm approximates the perturbation term $\boldsymbol{\Delta}_u(\boldsymbol{x}, \boldsymbol{u}, h)$. This proposed method requires neither the parameters nor the signs of the CEM.

V. NUMERICAL VALIDATIONS

In this section, numerical simulations are provided to demonstrate the effectiveness of the proposed approach by an aircraft attitude tracking problem accounting for uncertainties, actuator faults, sensing errors, and structural damage. The control variables are chosen as $\boldsymbol{y} = [\phi, \theta, \beta]^\mathsf{T}$, which contain the roll angle, pitch angle, and sideslip angle. The nonlinear flight dynamic model considering faults is represented as

$$\begin{cases} \dot{\boldsymbol{x}}_1 = \boldsymbol{f}_1(\boldsymbol{x}) + \boldsymbol{g}_1(\boldsymbol{x}_1)\boldsymbol{x}_2 \\ \dot{\boldsymbol{x}}_2 = (1-\kappa)(\boldsymbol{f}_2(\boldsymbol{x}) + \boldsymbol{g}_2(\boldsymbol{x})\boldsymbol{u}) + \kappa(\boldsymbol{f}_2'(\boldsymbol{x}) + \boldsymbol{g}_2'(\boldsymbol{x})\boldsymbol{u}) \end{cases} \tag{69}$$

where $\boldsymbol{x}^\mathsf{T} = [\boldsymbol{x}_1^\mathsf{T}, \boldsymbol{x}_2^\mathsf{T}]$; $\boldsymbol{x}_1 = [\phi, \theta, \beta]^\mathsf{T}$; $\boldsymbol{x}_2 = [p, q, r]^\mathsf{T}$ represents the rotational velocity of the body-fixed frame relative to the inertial frame; $\boldsymbol{u} = [\delta_a, \delta_e, \delta_r]^\mathsf{T}$ contains the deflections of the ailerons, elevator and rudder, respectively; $\kappa \in [0, 1]$ is an unit step function to denote sudden actuator fault or structure breakage. The specific expressions for the pre-fault dynamics $\boldsymbol{f}_1(\boldsymbol{x_1})$ and $\boldsymbol{g}_1(\boldsymbol{x}_1)$ can be found in [6]. The postfault functions $\boldsymbol{f}_2'(\boldsymbol{x})$ and $\boldsymbol{g}_2'(\boldsymbol{x})$ are modeled as in [10]. The relative degree of the system in (69) is $\boldsymbol{\rho} = [2, 2, 2]^\mathsf{T}$.

In reality, the time-varying CEM $\boldsymbol{\mathcal{B}}_0(\boldsymbol{x})$ of a faulty aircraft is very hard to be modeled accurately. Because the CEM $\boldsymbol{\mathcal{B}}_0(\boldsymbol{x})$ is a real square matrix, it can be decomposed as $\boldsymbol{\mathcal{B}}_0(\boldsymbol{x}) = \boldsymbol{\mathcal{B}}_s(\boldsymbol{x})\boldsymbol{\Lambda}\boldsymbol{U}(\boldsymbol{x})$.

The aircraft model used for evaluating the proposed method in Section IV is the public model of F-16 [38]. The initial states are set as in [10], i.e., $\boldsymbol{x}_1 = [0, 0, 0]^\circ$, $\boldsymbol{x}_2 = [0, 0, 0]^\circ/\mathrm{s}$. The sampling interval $h = 0.01$ s. In the simulations, the actuators are modeled as second-order systems with saturation limits [5, Table 2]. The maximum angular acceleration sensing bias is set as 0.25 rad/s^2. In addition, the power spectral density (PSD) height of the angular acceleration noise is set to 10^{-5}. Up to ten percent of parametric uncertainties are also added to the simulations. The control parameter values are given in Table I.

TABLE I
Control Parameters

Channel	INDI parameters		SMC parameters	
	$K_{i,0}$	$K_{i,1}$	$K_{s,i}$	γ_i
Roll, ϕ	15	5	1.5	0.25
Pitch, θ	15	5	1.5	0.25
Sideslip, β	9	3	0.5	0.25

TABLE II
Command Tracking Performance

Metrics		Ad-INDI	Obv-INDI	SMC-INDI
RMS	ϕ	0.1185	0.5382	0.2036
	θ	0.0452	0.4397	0.0177
	β	0.0414	0.0616	0.0252
$\|e\|_\infty$		0.0024	0.0071	0.0008
IAU		331.6568	318.2108	317.9278

During the aircraft attitude tracking task, the structural damage happens at $t = 5$ s, where the right wing lost 25% of its area; the entire left horizontal stabilator and a half of the vertical tail are also lost. Apart from these structural damage, actuator faults are added from $t = 10$ s. Specifically, the aileron lost 60% of its effectiveness; the elevator lost half of its the effectiveness; the rudder lost 40% of its effectiveness. Moreover, from $t = 10$ s, the right aileron runs away and get jammed at 15.05°. Also, the left elevator is jammed at $\bar{\delta}_{e_l} = -12.5^\circ$.

1) *Tracking Performance of the INDI-Based Control Methods:* The effectiveness of the three FTC augmentations (Section II.II-B) for the INDI control are first compared. To be specific, they are adaptive INDI (Ad-INDI), disturbance observer-augmented INDI (Obv-INDI), and sliding mode control-augmented INDI (SMC-INDI). The fault scenarios satisfy the condition in (15). Also, the correct control directions are first exposed to the controllers. To quantify the results, the root mean square (RMS) and the

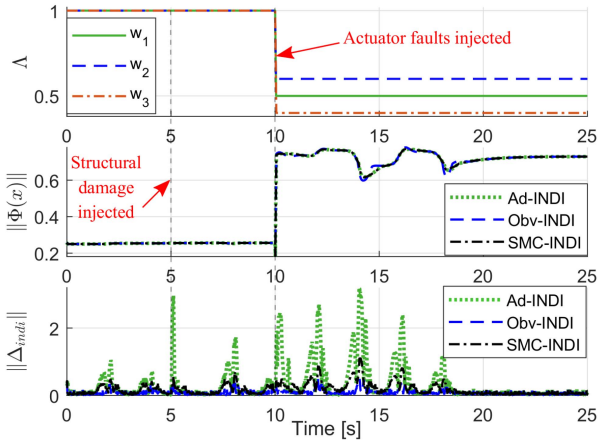

Fig. 1. Values of $\mathbf{\Lambda}$, the bounds of $\|\mathbf{\Phi}(\boldsymbol{x})\|$ and $\|\mathbf{\Delta}_{\text{indi}}\|$.

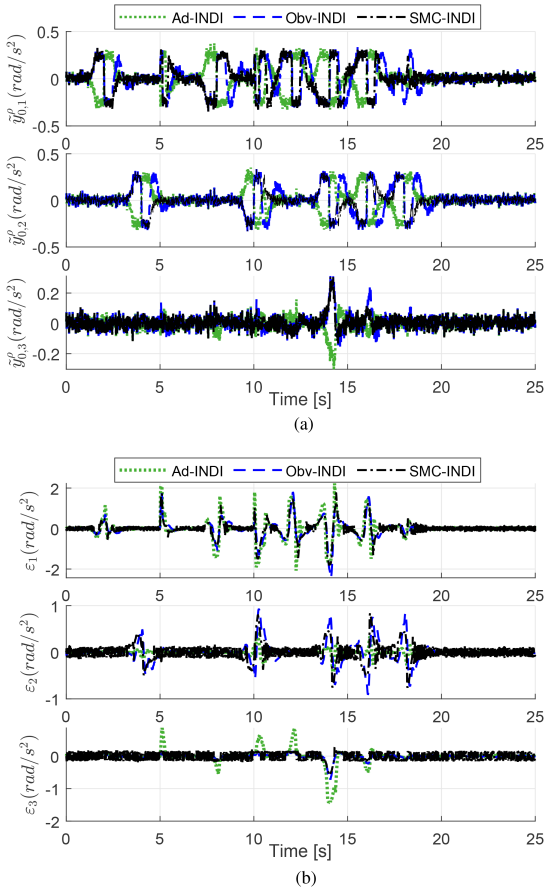

Fig. 2. Sensing error and the perturbation compensation error. (a) Sensing error. (b) Perturbation compensation error (Eq. (27)).

infinite norm of the tracking error, and the integral of control cost (IAU $= \sum_{i=1}^{3} \int_0^{t_f} |u_i(t)|\mathrm{d}t$) are shown in Table II.

The simulation results for the first scenario in which the uncertainties satisfying $\|\mathbf{\Phi}(x)\| < 1$ [see (15)] are illustrated in Figs. 1–3. Notice from Fig. 1 that the elevator, aileron and rudder faults are injected at 10 s. These faults are unknown to the controllers. The second subplot of Fig. 1 shows the impacts of actuator faults on $\|\mathbf{\Phi}(\boldsymbol{x})\|$. The residual cancellation error $\mathbf{\Delta}_{\text{indi}}$ is shown in the third subplot of

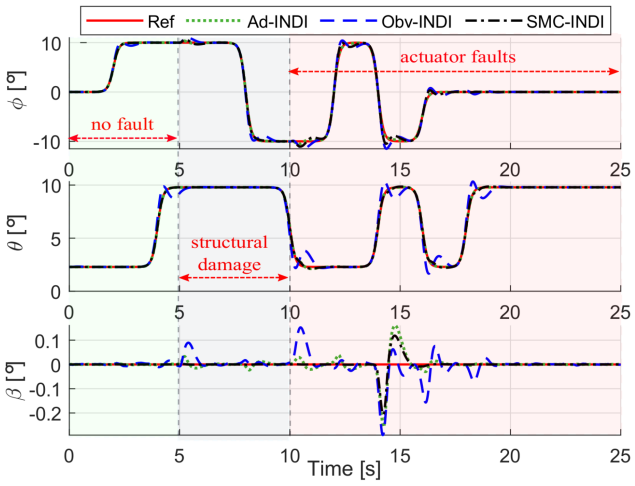

Fig. 3. Attitude tracking performance comparisons of Ad-INDI, Obv-INDI, and SMC-INDI.

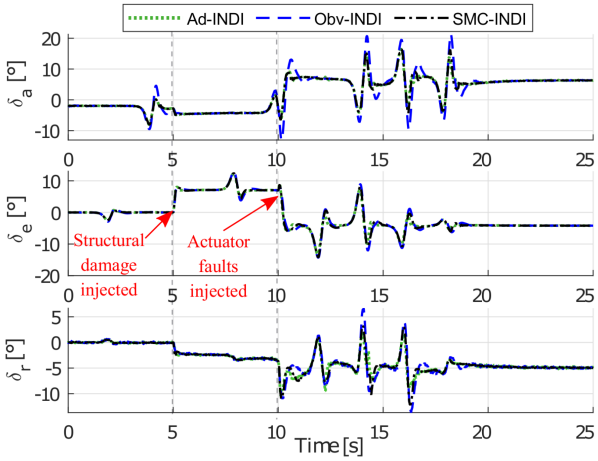

Fig. 4. Control inputs of Ad-INDI, Obv-INDI, and SMC-INDI.

Fig. 1; its variations are mainly induced by faults, damage, and command variations.

The simulated sensing errors are shown in Fig. 2(a). Fig. 2(b) shows the approximation errors of the term $\mathbf{\Delta}_{\text{indi}}$ [see (27)]. Fig. 3 plots the attitude tracking responses. It can be observed that the simulated sensing error, structural damage, and actuator faults can be tolerated by Ad-INDI, Obv-INDI, and SMC-INDI, which confirmed Theorem 1. It can also be seen from Fig. 3 and Table II that the SMC-INDI scheme tracks the references with the highest accuracy. The control actions illustrated in Fig. 4 are essential for command tracking and perturbation compensations. They are also smooth without chattering.

In the second simulation scenario, the diagonal entries of $\hat{\boldsymbol{\mathcal{B}}}(\boldsymbol{x})$ and $\boldsymbol{\mathcal{B}}(\boldsymbol{x})$ with opposite signs is tested. It can be seen from Fig. 5(a) that the actuation sign of the aileron is reversed at $t = 10$ s. As proven in Theorem 2, an incorrect estimation of control direction would break the control stability. This is verified in Fig. 5(b) as all the three INDI-based control schemes are unable to stabilize the aircraft, leading to unbounded tracking errors and closed-loop perturbations.

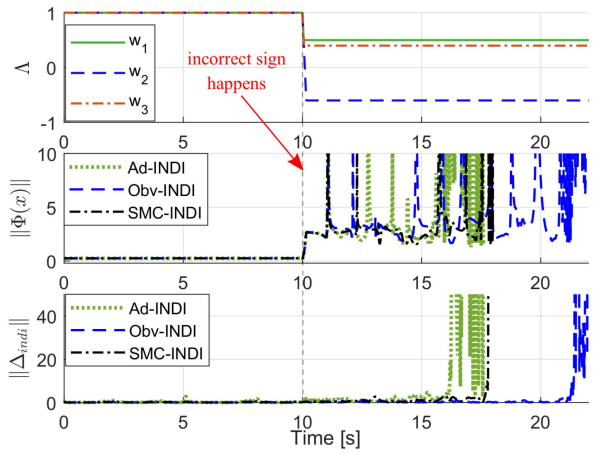

(a)

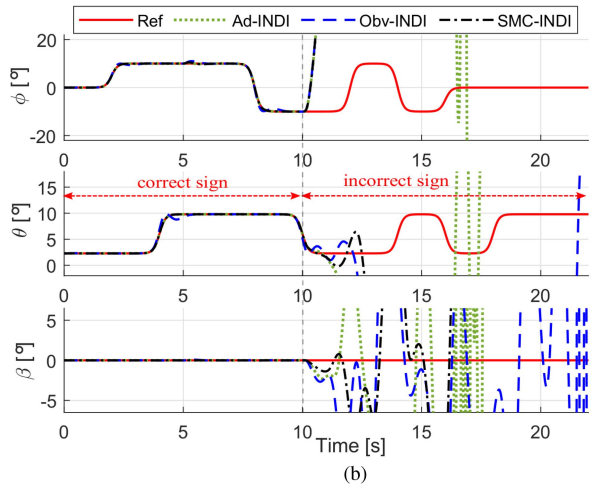

(b)

Fig. 5. Tracking performance of Ad-INDI, Obv-INDI, and SMC-INDI with incorrect control sign. (a) Control effectiveness faults $\mathbf{\Lambda}$, the bounds of $\|\mathbf{\Phi}(\boldsymbol{x})\|$ and $\|\mathbf{\Delta}_{\text{indi}}\|$. (b) Attitude.

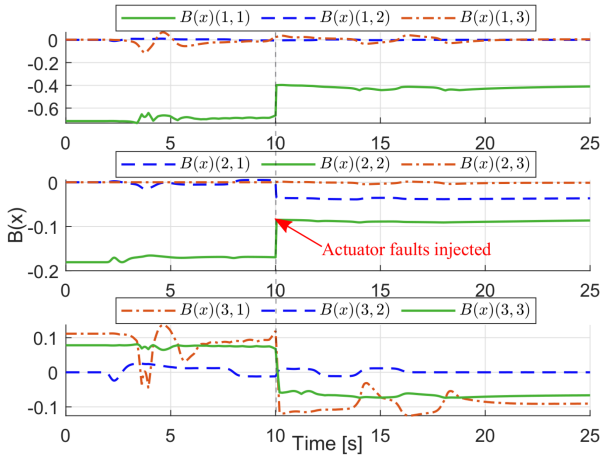

Fig. 6. Control effectiveness matrix $\boldsymbol{\mathcal{B}}(\boldsymbol{x})$.

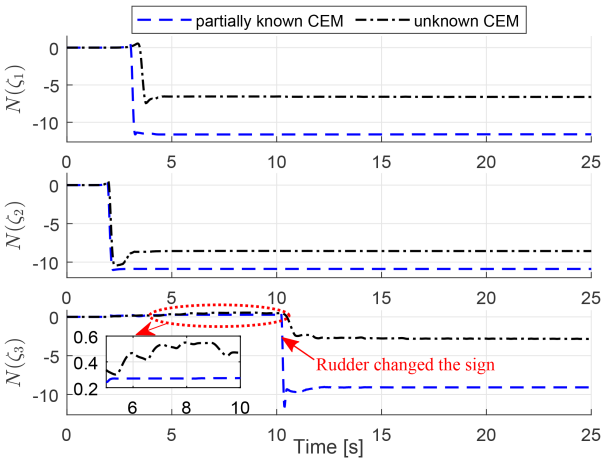

Fig. 7. Responses of the Nussbaum function $\mathcal{N}(\zeta)$.

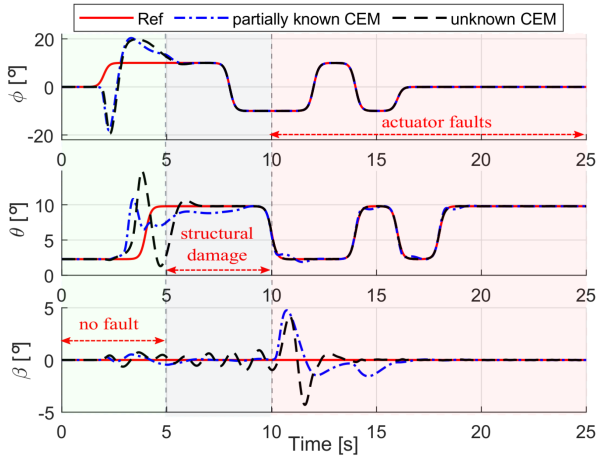

(a)

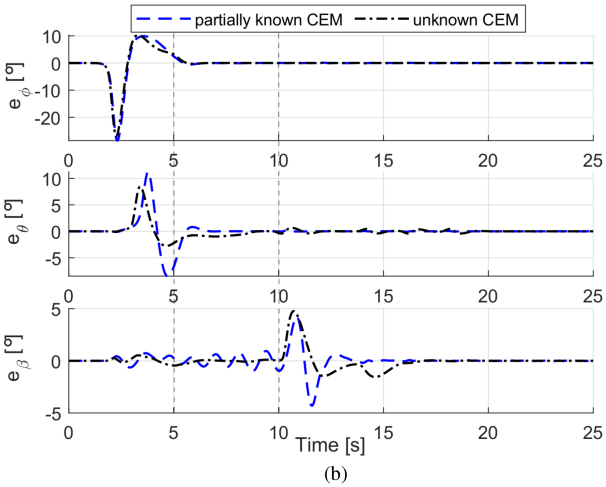

(b)

Fig. 8. Attitude tracking performance of N-INDI. (a) Attitude. (b) Tracking errors.

1) *Tracking Performance With Unknown Control Effectiveness:* In this section, simulations are performed for two different cases: 1) when the CEM $\boldsymbol{\mathcal{B}}_0(\boldsymbol{x})$ is partially known (only $\boldsymbol{B}_s$ is known while the control direction matrix $\mathbf{\Lambda}$ is unknown), the Nussbaum function-based adaptive incremental control law in (46) is applied; 2) when the CEM $\boldsymbol{\mathcal{B}}_0(\boldsymbol{x})$ is completely unknown, the Nussbaum function-based adaptive incremental control law in (60) is

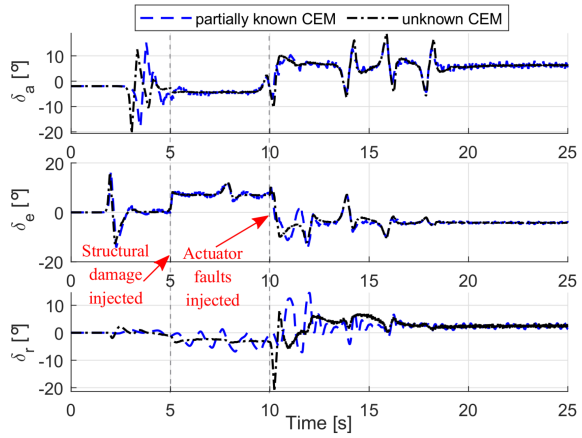

Fig. 9. Control inputs of N-INDI.

applied. The control parameters in (61) are set as: $\mu_i^j = 25$, $\rho_i^j = 0.01$.

The simulation results are shown in Figs. 6–9. The real CEM $\mathcal{B}(\boldsymbol{x})$ is illustrated in Fig. 6. It can be seen that sudden actuator faults induce large variations in the diagonal elements of $\mathcal{B}(\boldsymbol{x})$; in particular, the third diagonal entry (corresponds to the rudder) changed it sign at $t = 10$ s. Fig. 7 shows that the Nussbaum gains swiftly adapt to match the real control directions.

The attitude tracking responses are illustrated in Fig. 8. Even without the control sign information, by only knowing $\boldsymbol{B}_s$, the proposed control law in (46) can tolerate all the faults while continuing in executing the tracking task. Furthermore, even when the CEM is completely unknown, the proposed control law in (60) can still accomplish the FTC tracking task. These verify Theorems 3 and 4. The control inputs are shown in Fig. 9. It can be observed that a short period of oscillations happened after the control reversal, indicating that the Nussbaum function-based adaptive laws are searching for the correct control directions.

VI. CONCLUSION

This article solves the MIMO nonlinear system FTC problem, especially for the case of unknown control effectiveness. It first unifies the Lyapunov-based stability proof for the MIMO nonlinear perturbed system using the nonlinear incremental control framework, regardless of the perturbation compensation achieved by whether adaptive, disturbance observer or sliding-mode augmentations. Then, this article reveals that all of the existing nonlinear incremental control methods depend on a critical sufficiently condition on the CEM, and this condition is essentially identical to the matching condition in dynamic inversion-based adaptive control design. However, it is proved in this article that this condition is violated when the control direction is unknown; thus, neither the boundedness of the closed-loop perturbations nor the stability can be guaranteed no matter which perturbation compensation techniques are implemented. Therefore, this article proposes two Nussbaum function-based adaptive nonlinear incremental control methods for partially unknown CEM and completely unknown CEM, respectively. Lyapunov-based stability analysis and numerical simulations have proved the effectiveness of the proposed methods. To be specific, the Nussbaum function identifies the control direction online while the adaptive control algorithm approximates and compensates for the perturbations, guaranteeing closed-loop stability in a flight tracking task encountering parametric uncertainties, actuator faults, sensing errors, structural damage, and inversed control directions.

REFERENCES

[1] S. Sieberling, Q. Chu, and J. Mulder, "Robust flight control using incremental nonlinear dynamic inversion and angular acceleration prediction," *J. Guidance, Control, Dyn.*, vol. 33, no. 6, pp. 1732–1742, 2010.

[2] Q. Hu, X. Shao, and W. Chen, "Robust fault-tolerant tracking control for spacecraft proximity operations using time-varying sliding mode," *IEEE Trans. Aerosp. Electron. Syst.*, vol. 54, no. 1, pp. 2–17, Feb. 2018.

[3] K. Rudin, G. J. J. Ducard, and R. Y. Siegwart, "Active fault-tolerant control with imperfect fault detection information: Applications to uavs," *IEEE Trans. Aerosp. Electron. Syst.*, vol. 56, no. 4, pp. 2792–2805, Aug. 2020.

[4] H. Park and Y. Kim, "Adaptive fault tolerant flight control for input redundant systems using a nonlinear reference model," *IEEE Trans. Aerosp. Electron. Syst.*, vol. 57, no. 5, pp. 3337–3356, Oct. 2021.

[5] X. Wang, E. van Kampen, Q. Chu, and P. Lu, "Incremental sliding-mode fault-tolerant flight control," *J. Guidance, Control, Dyn.*, vol. 42, no. 2, pp. 244–259, 2019.

[6] E. J. Smeur, Q. Chu, and G. C. de Croon, "Adaptive incremental nonlinear dynamic inversion for attitude control of micro air vehicles," *J. Guidance, Control, Dyn.*, vol. 39, no. 3, pp. 450–461, 2016.

[7] X. Wang, S. Sun, E. van Kampen, and Q. Chu, "Quadrotor fault tolerant incremental sliding mode control driven by sliding mode disturbance observers," *Aerosp. Sci. Technol.*, vol. 87, pp. 417–430, 2019.

[8] F. Grondman, G. Looye, R. O. Kuchar, Q. Chu, and E. Van Kampen, "Design and flight testing of incremental nonlinear dynamic inversion-based control laws for a passenger aircraft," in *Proc. AIAA Guidance, Navigation, Control Conf.*, 2018, Art. no. 0385.

[9] A. Zolghadri, "On flight operational issues management: Past, present and future," *Annu. Rev. Control*, vol. 45, pp. 41–51, 2018.

[10] J. Chang, R. De Breuker, and X. Wang, "Discrete-time design and stability analysis for nonlinear incremental fault-tolerant flight control," in *Proc. AIAA SCITECH 2022 Forum*, 2022, Paper no. 2034.

[11] P. Bhardwaj, V. S. Akkinapalli, J. Zhang, S. Saboo, and F. Holzapfel, "Adaptive augmentation of incremental nonlinear dynamic inversion controller for an extended f-16 model," in *Proc. AIAA Scitech 2019 Forum*, 2019, Paper no. 1923.

[12] Y. Li, X. Liu, P. Lu, Q. He, R. Ming, and W. Zhang, "Angular acceleration estimation-based incremental nonlinear dynamic inversion for robust flight control," *Control Eng. Pract.*, vol. 117, 2021, Art. no. 104938.

[13] B. J. Jeon, M. G. Seo, H. S. Shin, and A. Tsourdos, "Understandings of classical and incremental backstepping controllers with model uncertainties," *IEEE Trans. Aerosp. Electron. Syst.*, vol. 56, no. 4, pp. 2628–2641, Aug. 2020.

[14] J. B. R. Rose and G. Jinu, "Influence of aeroelastic control reversal problem in the airplane lateral stability modes," in *Proc. Inst. Mech. Engineers, Part G, J. Aerosp. Eng.*, vol. 229, no. 3, pp. 517–533, 2015.

[15] "Aviation incident final report-cen15ia079, st. louis, mo" National Transportation Safety Board, St Louis, MO, Int. Civil Aviation Org. (ICAO), *Tech. Rep.*, Mar., 2015.

[16] R. K. Dismukes, B. A. Berman, and L. Loukopoulos, *The Limits of Expertise: Rethinking Pilot Error and the Causes of Airline Accidents. Routledge*, Aldershot, U.K., Ashgate Publishing Limited, 2007.

[17] A. J. Peixoto, T. R. Oliveira, D. Pereira-Dias, and J. C. Monteiro, "Multivariable extremum-seeking by periodic switching functions with application to raman optical amplifiers," *Control Eng. Pract.*, vol. 96, 2020, Art. no. 104278.
[18] Z. Guo, T. R. Oliveira, J. Guo, and Z. Wang, "Performance-guaranteed adaptive asymptotic tracking for nonlinear systems with unknown sign-switching control direction," *IEEE Trans. Autom. Control*, 2022, doi: 10.1109/TAC.2022.3144661.
[19] H. E. Psillakis, "Consensus in networks of agents with unknown high-frequency gain signs and switching topology," *IEEE Trans. Autom. Control*, vol. 62, no. 8, pp. 3993–3998, Aug. 2017.
[20] T. R. Oliveira, A. J. Peixoto, and E. V. Nunes, "Binary robust adaptive control with monitoring functions for systems under unknown high-frequency-gain sign, parametric uncertainties and unmodeled dynamics," *Int. J. Adaptive Control Signal Process.*, vol. 30, no. 8–10, pp. 1184–1202, 2016.
[21] T. R. Oliveira, A. J. Peixoto, and L. Hsu, "Sliding mode control of uncertain multivariable nonlinear systems with unknown control direction via switching and monitoring function," *IEEE Trans. Autom. Control*, vol. 55, no. 4, pp. 1028–1034, Apr. 2010.
[22] Y. Ma, H. Ren, G. Tao, and B. Jiang, "Adaptive compensation for actuation sign faults of flexible spacecraft," *IEEE Trans. Aerosp. Electron. Syst.*, vol. 57, no. 2, pp. 1288–1300, Apr. 2021.
[23] J. Kaloust and Z. Qu, "Continuous robust control design for nonlinear uncertain systems without a priori knowledge of control direction," *IEEE Trans. Autom. Control*, vol. 40, no. 2, pp. 276–282, Feb. 1995.
[24] H. Chen, J. Zhou, M. Zhou, and B. Zhao, "Nussbaum gain adaptive control scheme for moving mass reentry hypersonic vehicle with actuator saturation," *Aerosp. Sci. Technol.*, vol. 91, pp. 357–371, 2019.
[25] B. Xu, R. Qi, and B. Jiang, "Adaptive fault-tolerant control for hsv with unknown control direction," *IEEE Trans. Aerosp. Electron. Syst.*, vol. 55, no. 6, pp. 2743–2758, Dec. 2019.
[26] C. Wang, C. Wen, and L. Guo, "Multivariable adaptive control with unknown signs of the high-frequency gain matrix using novel nussbaum functions," *Automatica*, vol. 111, 2020, Art. no. 108618.
[27] W. Chen, X. Li, W. Ren, and C. Wen, "Adaptive consensus of multi-agent systems with unknown identical control directions based on a novel nussbaum-type function," *IEEE Trans. Autom. Control*, vol. 59, no. 7, pp. 1887–1892, Jul. 2014.
[28] M. Lv, W. Yu, J. Cao, and S. Baldi, "Consensus in high-power multiagent systems with mixed unknown control directions via hybrid nussbaum-based control," *IEEE Trans. Cybern.*, vol. 52, no. 6, pp. 5184–5196, Jun. 2020.
[29] X. Wang, E. van Kampen, Q. Chu, and P. Lu, "Stability analysis for incremental nonlinear dynamic inversion control," *J. Guidance, Control, Dyn.*, vol. 42, no. 5, pp. 1116–1129, 2019.
[30] Z. Yu and J. L. Crassidis, "Accelerometer bias calibration using attitude and angular velocity information," *J. Guidance, Control, Dyn.*, vol. 39, no. 4, pp. 741–753, 2016.
[31] S. Kim, V. Tadiparthi, and R. Bhattacharya, "Computationally efficient attitude estimation with extended $\mathcal{H}_2$ filtering," *J. Guidance, Control, Dyn.*, vol. 44, no. 2, pp. 418–427, 2021.
[32] J. Zhou, J. Chang, and Z. Guo, "A fault-tolerant control scheme within adaptive disturbance observer for hypersonic vehicle," *Proc. Inst. Mech. Engineers, Part G, J. Aerosp. Eng.*, vol. 233, no. 3, pp. 1071–1088, 2019.
[33] J. A. Lewis and E. N. Johnson, "Gain switching control law for dynamic inversion based adaptive control with unknown sign of control effectiveness," in *Proc. AIAA Scitech 2021 Forum*, 2021, pp. 1–25.
[34] W. Su, S. Drakunov, and U. Ozguner, "An o (t^2) boundary layer in sliding mode for sampled-data systems," *IEEE Trans. Autom. Control*, vol. 45, pp. 482–4853, Mar. 2000.
[35] Z. Chen, "Nussbaum functions in adaptive control with time-varying unknown control coefficients," *Automatica*, vol. 102, pp. 72–79, 2019.
[36] R. R. Costa, L. Hsu, A. K. Imai, and P. Kokotović, "Lyapunov-based adaptive control of mimo systems," *Automatica*, vol. 39, no. 7, pp. 1251–1257, 2003.
[37] A. Boulkroune, M. M'Saad, and H. Chekireb, "Design of a fuzzy adaptive controller for mimo nonlinear time-delay systems with unknown actuator nonlinearities and unknown control direction," *Inf. Sci.*, vol. 180, no. 24, pp. 5041–5059, 2010.
[38] L. T. Nguyen, Simulator study of stall/post-stall characteristics of a fighter airplane with relaxed longitudinal static stability, vol. 12854, *Nat. Aeronaut. Space Admin.*, Hampton, VA, US, NASA Langley Research Center, 1979.

Jing Chang received the M.E. and Ph.D. degrees in navigation guidance and control from Northwestern Polytechnical University, Xi'an, China, in 2013 and 2018, respectively.

Since June 2018, she has become an Assistant Professor with the School of Aerospace Science and Technology of Xidian University. From January 2021 to August 2022, she is a Visiting Researcher with the Department of Aerospace Structures and Materials, Delft University of Technology, Delft, The Netherland. Her research interests include fault diagnosis, fault tolerant control, nonlinear control, and flight control.

Roeland De Breuker received the Ph.D. degree in the aerospace engineering from Delft University of Technology, Delft, the Netherlands, in 2011.

He joined the faculty of Aerospace Engineering in Delft as an Assistant Professor in 2011 and became Associate Professor in 2017. He has been visiting Researcher with Clarkson University, Potsdam, NY, USA and visiting Professor with Airbus Innovations, Germany.

Dr. Breuker is the Associate Fellow of the American Institute of Aeronautics and Astronautics. He also serves as the Associate Editor of the *Journal of Fluids and Structures and the Journal of Intelligent Material Systems and Structures*.

Xuerui Wang (Member, IEEE), received the B.S. degree in aerospace engineering from Beijing University of Aeronautics and Astronautics, Beijing, China, in 2014, and the Ph.D. degree in aerospace engineering from Delft University of Technology (TU Delft), Delft, the Netherlands, in 2019.

From May 2019 to May 2020, she was a Postdoctoral Researcher with the Smart and Aeroelastic Structure Laboratory in TU Delft, Delft, The Netherland. Since May 2020, she has become an Assistant Professor with the Faculty of Aerospace Engineering, TU Delft. Her tenure track program is co-funded by the Department of Control and Operations and the Department of Aerospace Structures and Materials. Her research interests include nonlinear control, aeroelasticity, aerial robotics, and active morphing structures.